the outcrops as well as MJE-1 and MJE-3, still exists in this hole discontinuously.

The concealed "network" vein zone below the mineralized Zone A, which was confirmed by MJE-1 and MJE-3 last year, is considered to continue to this hole and to correspond with extremely fine-grained and/or fine-grained pyrite-(chalcopyrite)-(chlorite)-secondary biotite-quartz veinlet sections: the 289.10 to 290.10 m, 312.90 to 312.91 m, 315.30 to 315.35 m. 319.80 to 320.80 m, 349.00 to 349.40 m, 350.30 to 351.20 m, sections. The mineralized zone branches, and shows the feature of the outer limit portion as a whole.

On the other hand, the "dissemination" zone which extends over this entire area centering in the mineralized Zone B, is observed in this hole between 270 and 340 m in depth centering on the 310 to 320 m section. The quantity of chalcopyrite is generally less than that at the outcrops of Esperanza valley, and dissemination in host rock is few in veins. These facts show that this hole has penetrated near the northeastern end of the mineralized Zone B.

The deep IP anomalous zone of geophysical survey is proved to be an "dissemination" of sulfide mineralized zone mentioned above.

1-4 Consideration of survey results in El Torneado zone

Survey in this area has been performed for two years, with detailed geological survey, CSAMT geophysical survey, Bore Hole IP method electric exploration, and drilling survey. As results, the following facts were found in the El Torneado mineralized zone.

The El Torneado mineralized zone consists of two mineralized zones: "dissemination" mineralized zone and "network" vein mineralized zone which are different each other in occurrence and properties. The former extends over a range of 400 m x 400 m, and the latter extends in NNE-SSW direction and is distributed in a scale of 40 to 70 m wide and 70 to 350 m in extension in the distribution area of the former. The former is cut by the latter, and the former has been mineralized earlier than the latter.

The "dissemination" zone is mineralized as the same features and properties as those of other porphyry copper type mineralized zone in the Bolivar area. From the central part of the mineralized zone to outer part, the tendency of a orderly change is observed in the paragenesis, features, alteration, etc. of sulfide minerals.

In the central portion of the mineralized zone, chalcopyrite and pyrite are disseminated not only in veinlets, but also in host rock. The sulfide minerals are entirely disseminated in quartz and plagioclase portions as well as mafic mineral portion. Alteration of host rocks comprises noticeable secondary biotitization and chloritization.

Epidote tends to increase where chalcopyrite abounds. Outer part of the mineralized zone, the quantity of sulfide minerals generally decrease, and the chalcopyrite/pyrite ratio reduces gradually. The chalcopyrite is not observed as dissemination in host rocks, but is limitted in veinlets only. Further outside, sulfide minerals in veinlets are only chalcopyrite. Dissemination of sulfide minerals in host rocks is limitted in the portion of mafic minerals. For alteration of host rocks, moreover, secondary biotite is not observed, but only weak chloritization. Further outside, enters into an unaltered zone. This tendency is also observed downward of the mineralized zone at the outside edge of the mineralized zone.

The "network" vein zone is distributed in NNE-SSW direction within the area of the "dissemination" zone. This type of mineralization is not observed in other porphyry copper type mineralized zones in the Bolivar area. Also in this mineralized zone, the tendency of a orderly change is observed from the central part of the mineralized zone to the outer part.

In the central part of the mineralized zone, the breccia structure of host rock has noticeably developed, and the interstices of breccias are filled with a network form chalcopyrite-pyrite-(molybdenite)-(pyrrhotite)-secondary biotite-chlo-rite-quartz veins. At the outer part, breccias are scarcely developed, and sulfide minerals in network veins decreased and veins thinned into veinlets. Vertically the lower part of this mineralized zone transited to shearing fracture zone, and the networked veins changed into fine-grained pyrite-secondary biotite-(chlorite)-quartz veins existing along the fracture surface.

For alteration of host rocks, chloritization, silicification and secondary biotitization are observed along veins. In the central part of the mineralized zone, this alteration tends to be strong, and comparatively wide. The outer and deeper, the weaker and narrower the alteration becomes and finally to just sericitization, which is observed at ground surface spreading over the entire mineralized zone horizontally but not vertically.

It is considered that the principal mineralized zone of the El Torneado zone has been eroded and that the lower part of the mineralized zone are exposed at the current ground surface, based on the following facts: (1) horizontal and vertical changes of the"dissemination" zone as mentioned above: (2) MJE-4 and MJE-5 holes penetrated the lower limit of the "network" vein zone: (3)the "dissemination" zone is also about reaching the lower limit of mineralization.

Chapter 2 Osohuayco zone, Balzapamba area

2-1 Geology and mineralization

Geology and distribution of mineral showings are shown in Fig.II-2-1.

The geology in the area consists of the Macuchi Formation and granitic rocks. The Macuchi Formation comprises member An-1, which is distributed around mountains and hills in the southern part of the survey area. On the other hand, granitic rocks comprises biotite-hornblende granodiorite, which is distributed along valleys and mid-slops in the northern part.The member An-1 consists of andesite lava and its tuffs with intercalation of thin mud beds locally. Three layers of andesitic tuffs are recognized in this area and crop out as banded figures with NE in strike and 10° to 45° SE in dip. At the contact with granodiorite, rocks metamorphosed to hornfels.

Two mineralized zones are recognized in the area: one is northwest mineralized zone in granodiorite; and the other is south mineralized zone in the Macuchi Formation.

The mineralized zones in grandiorite are of chalcopyrite-pyrite-chlorite-quartz veinlets and sulfide dissemination. Host rocks are affected by chloritization and silicification. The scale of the mineralized zone is estimated to be about 100 m wide and 200 m long. The assay results of dissemination ore sample shows 0.08 % in Cu.

The mineralized zone in the Macuchi Formation is of "dissemination" zone consisting of chalcopyrite-pyrite-chalcocite-glossular-quartz vein (1 to 10 cm wide) locally, which are scattered along the bedding plane of tuff-member of the Macuchi Formation. The tuffs are affected by silicification generally and skarnization locally.

Mineralization is observed in the lower most tuff-member and in the middle member. The former mineralized zones are observed at three places: one is on the ridge line; the others are at the rivers in the east and west of the ridge. This mineralized zone contunue for about 350 m to the strike side with a width of 2 to 10 m. The assay result of chipped ore samples taken from eastern river shows 0.4 g/t in Au, 27.8 g/t in Ag and 2.60 % in Cu. The latter mineralized zone continues for about 600m with a width of 10 m. General strike and dip of these mineralized zones is NE and 20°SE respectively.

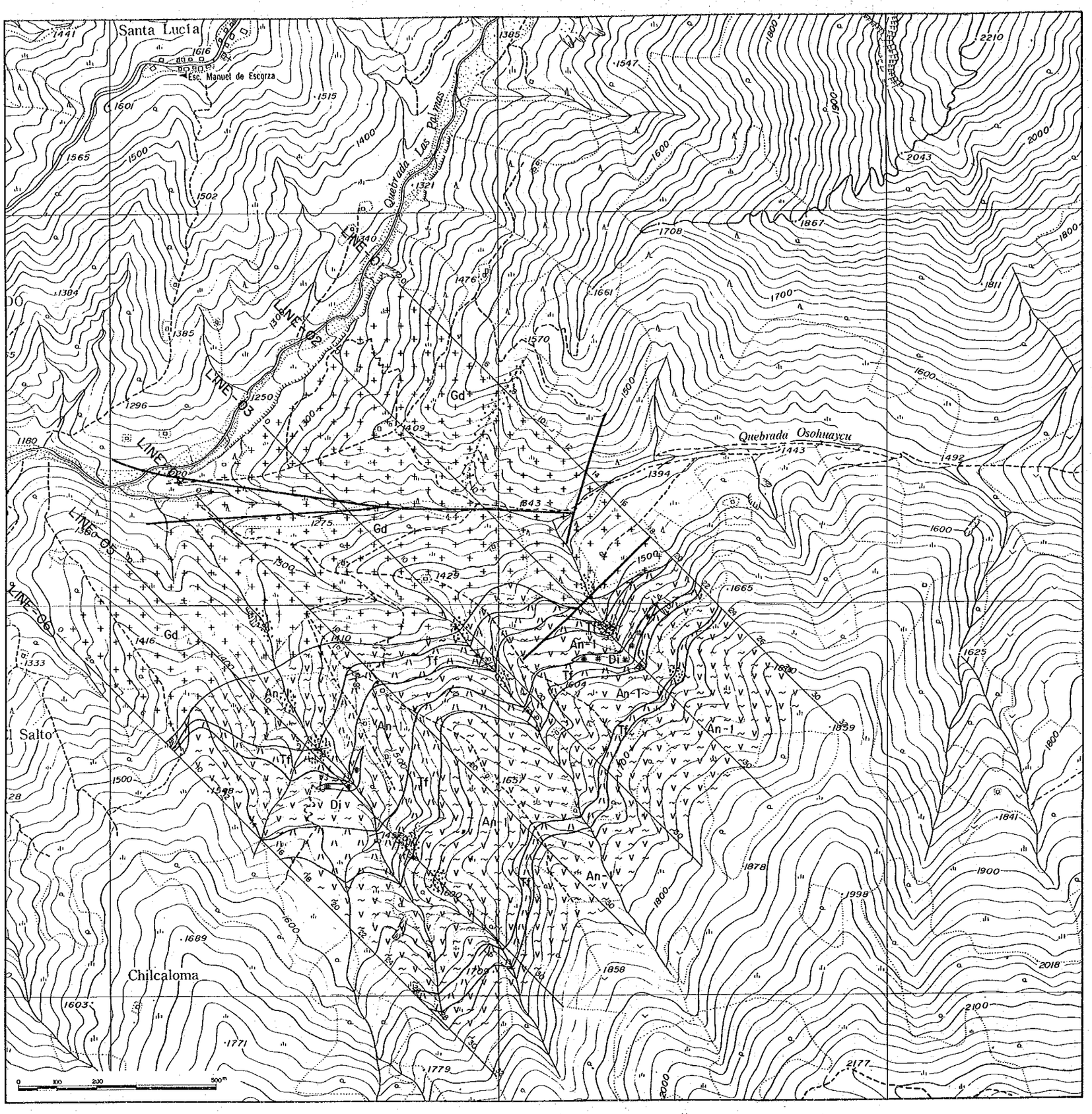

LEGEND

Cretaceous Macuchi Formation
- Tf — Andesitic to quartz-bg. andesitic pyroclastics (D Member)
- An-I — Andesite lava with its pyroclastics and sediment (Tf), and hornfels (A Member)

Intrusive Rocks
- Gd — Granodiorite
- Di — Melanocratic diorite dyke

- Dip and strike of bedding plane
- Geological boundary
- Fault
- Mineralized zone (Presumed)
- Vein

Fig. II–2–1 Geological map of the Osohuayco, Balzapamba area

2-2 Geophysical survey

2-2-1 Purpose of survey

The purpose of this survey is to clarify the lateral and vertical extension of the mineralization detected by the Phase I Survey. To meet the above, an investigation of electrical structure of the area was carried out by clarifying the distribution of IP anomalies in the survey area by means of a conventional IP method.

2-2-2 Survey method

(1) IP method

An IP (Induced Polarization) method is a geophysical technique that measures the polarization effects caused by the electrochemical nature of the minerals and rocks. This method has been mainly utilized for detecting sulphide deposits.

There exist four measuring methods to observe an IP phenomenon, i.e.,

1) Frequency-domain

When using the frequency-domain method, the magnitude of the IP phenomenon is expressed by the parameter called Frequency Effect (FE) which is proportional to the resistivity difference at two frequencies.

2) Time-domain

In this method, the magnitude of the IP effect is expressed by the Chargeability which is determined by observing the transient voltage curve after the electric current is turned off.

3) Phase-domain

The magnitude of the IP phenomenon in the phase-domain method is expressed in terms of the difference of the phase angle between the transmitted and received signals.

4) Spectral IP

The magnitude of the IP phenomenon is here expressed as the normalized amplitude and phase in each frequency referred to the lowest frequency among a wide variation of frequencies.

(2) Measurement method

The measurements were done by using the frequency-domain method at the frequencies of 3.0Hz and 0.3Hz and adopting a dipole-dipole electrode configuration with a separation factor n from 1 to 5.

Based upon the geological structure, six survey lines of 1600m each in length were set along a NW-SE direction with a 250m line spacing. The numbering of the points were set one by one from 0 to 32 with a 50m interval from the northwest end of each line and the measurements were done every 100m spacing with a 100m potential electrode.

The location of survey lines are illustrated in Fig.II-2-2.

(3) Survey instruments

Instruments used for the conventional IP survey were manufactured in Japan, with the exception of an engine generator which was manufactured in Canada, as shown below.

Equipment	Model	Specification	Quantity
IP Transmitter	CH-T7802	2.5A, 800V	1
IP Receiver	CH-R7802		1
IP Checker	522A		1
Engine Generator	GPU-2000	2kw, 150V, 400Hz	1
Electrode Remote Controller	CH-60A	64ch	1
Transceiver	ICB-660	0.5W	6

2-2-3 Analysis method

Fig.II-2-3 shows a procedure for data analysis.

(1) Calculation of apparent resistivity and frequency

The measurement is conducted by supplying electric current (Iac) at 3.0Hz into the ground through a pair of current electrodes (C1,C2) and detecting the corresponding potential difference (Vac) with a pair of potential electrodes (P1,P2).

The apparent resistivity (APR) of the ground is calculated by applying the measured potential difference to the following equation:

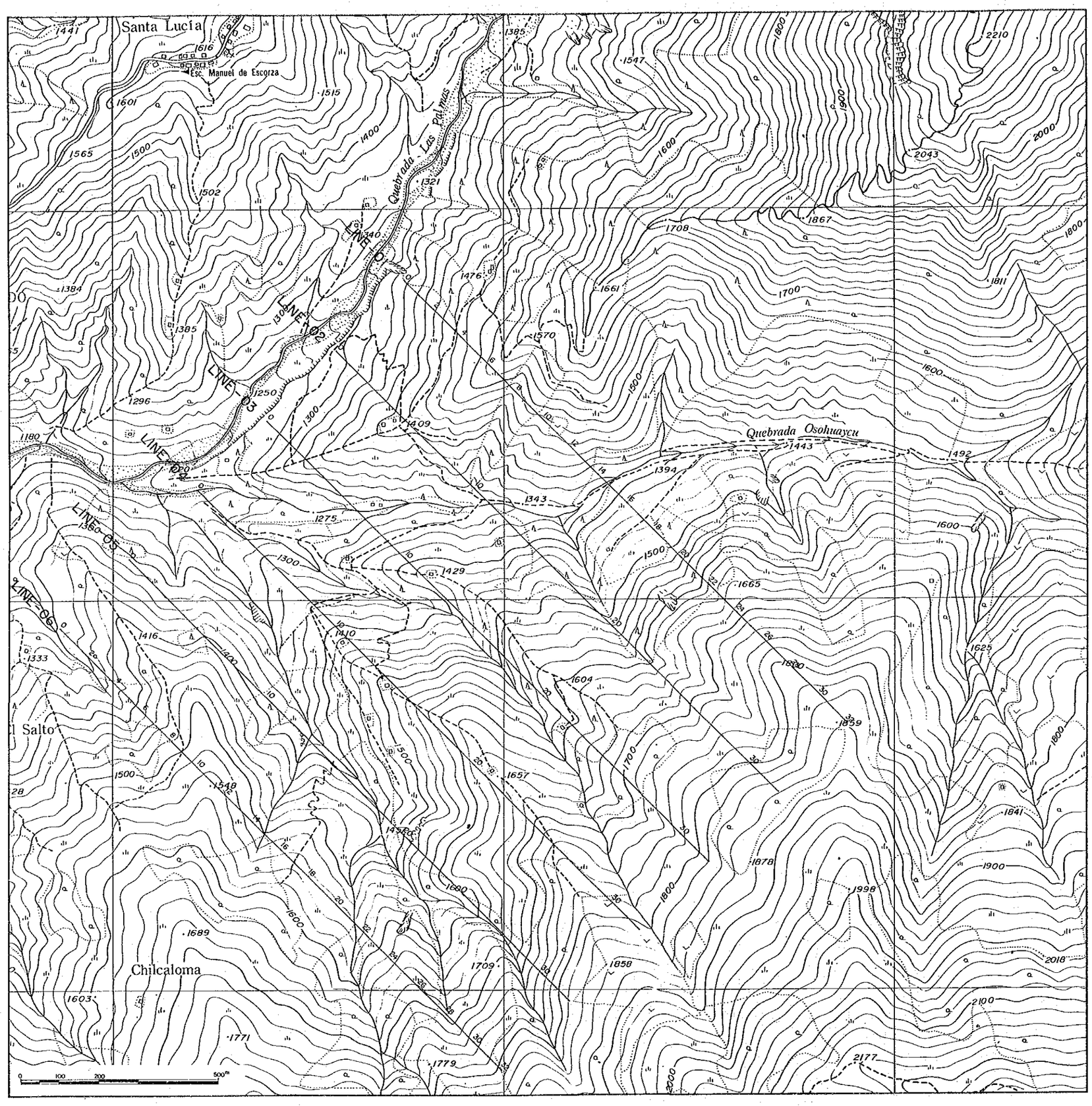

Fig. II–2–2 Location map of IP survey lines of the Osohuayco, Balzapamba area

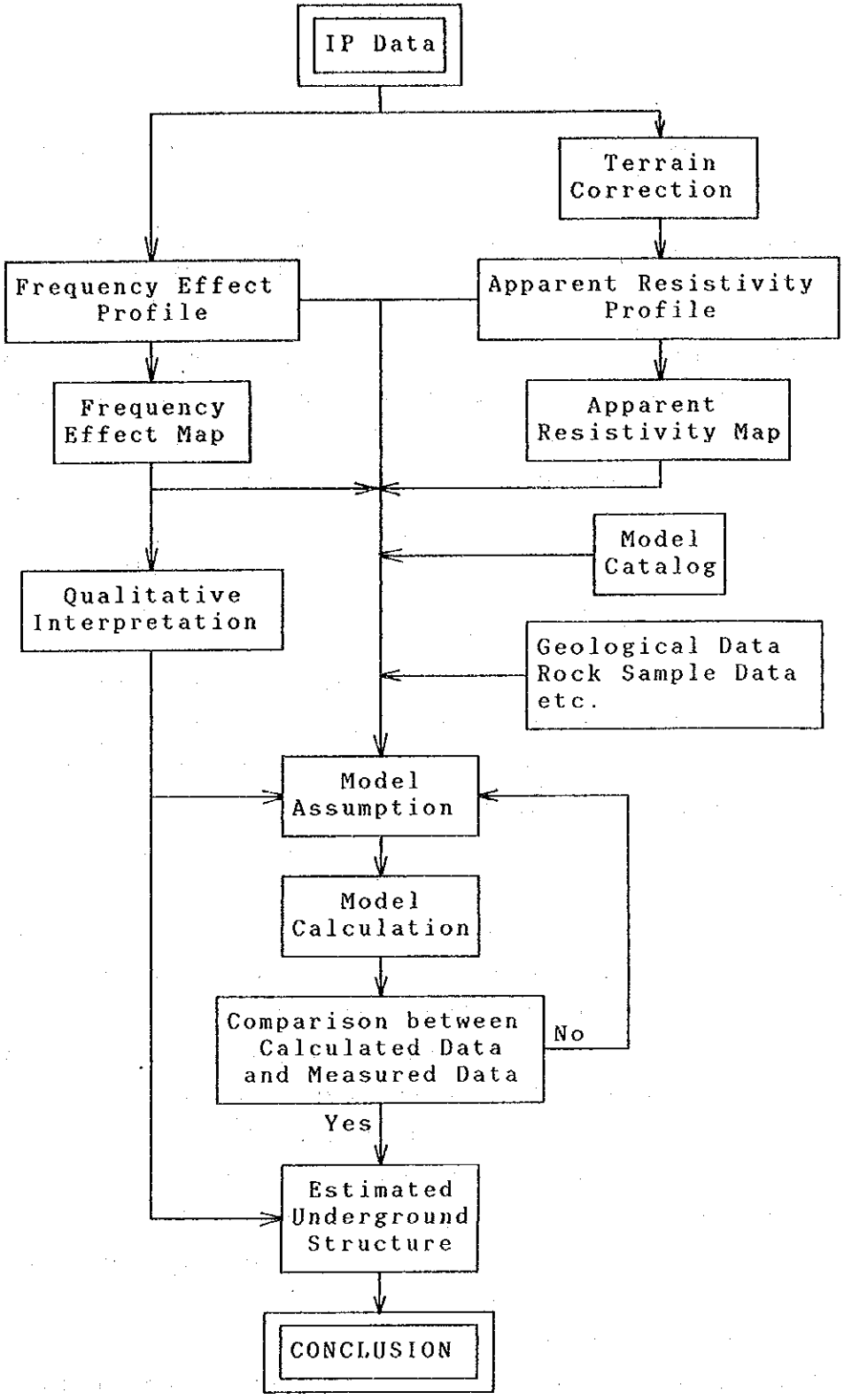

Fig. II–2–3 Flow chart of IP data analysis

$$\rho_{AC} = K \cdot \frac{V_{AC}}{I_{AC}} \quad (\Omega \cdot m)$$

K is a geometric factor which depends on the electrodic configuration utilized.

$$K = 2\pi / \left(\frac{1}{C_1 P_1} - \frac{1}{C_1 P_2} - \frac{1}{C_2 P_1} + \frac{1}{C_2 P_2} \right)$$

After reading the potential difference Vac at 3.0 Hz, the frequency is changed to 0.3Hz and the current is kept constant. The frequency effect (FE) can then be directly read by a meter of a receiver panel and calculated by the following formula, which is also a function of the change in resistivity as the frequency is changed.

$$FE = \frac{V_{DC} - V_{AC}}{V_{AC}} \times 100 = \frac{\rho_{DC} - \rho_{AC}}{\rho_{AC}} \times 100 \quad (\%)$$

The value of APR and FE are plotted at the intersection of lines extending downward at 45° angles from the transmitter and receiver midpoints. Since the depth of plotting does not represent the physical property with depth, this pseudo-section does not give a true section of the subsurface distribution of the IP effect.

(2) Terrain correction

APR is affected by topography depending on the location of electrodes, even if the terrain was homogeneous, as described in previous Chapters. For example, for the case of a dipole-dipole configuration, APR appears to be high beneath a hill and low beneath a valley. On the other hand, FE is less affected by topography because it is rather proportional to the ratio of resistivity differences at two frequencies.

As the topography of the survey area is comparatively steep and rugged, the correction was performed for all survey lines by means of a finite element method assuming a two dimensional half space topography.

The pseudo-sections and plan maps were drawn using the topography corrected values.

(3) Electrical measurement of rock samples

Electrical measurements on rock samples were carried out in order to determine the actual electrical properties of rocks distributed on the survey area.

The rocks collected from the surface were formed into a cubic shape and their

measurements realized in water saturated condition after the rocks were soaked in water during ten days.

The resistivities of the rock sample are calculated by the following equation:

$$\rho = \frac{a_1 \times a_2}{\ell} \times \frac{V}{I}$$

ℓ : thickness of sample (m)

a_1, a_2 : width of sample (m)

V : potential difference (V)

I : electric current (A)

As same as for the case of field survey, FE was calculated by using the resistivity differences at 0.3Hz and 3.0Hz.

(4) Simulation analysis

As described in item 1-2-3 of Chapter 1, model simulations due to a dipole-dipole configuration were done to clarify the underground physical structure.

2-2-4 Results of survey and analysis

Apparent resistivity values observed on Osohuayco Zone range from 122 to 5,960 Ohm-m. For convenience in this report, the resistivity values are classified into three categories, i.e., low resistivity for those values less than 650 Ohm-m, medium resistivity for values ranging from 650 to 1,500 Ohm-m and high resistivity for bigger than 1,500 Ohm-m.

As the FE values present also a wide variation between 2.5% and 22%, they also, for convenience, will be classified into the following four categories; high FE for values bigger than 8%, medium high FE for values from 6 to 8%, medium FE for values ranging between 4 and 6%, and low FE for values less than 4%.

In general, apparent resistivity obtained from this method are considered to correspond well with the geological formation in the survey area. In this area, the results of the survey reflects especially well alteration processes on the rock, such as argillization and silicification. For instant, low resistivity reflects mineralization and/or argillization in fault zones, while high resistivity reflects silicification. On the other hand, FE values indicate sulphide mineral dissemination such as chalcopyrite and

pyrite, reflecting their dissemination density.

The apparent resistivity values shown in plan maps and sections were all corrected for topographic effects.

(1) Results of electric measurement of rocks

In Osohuayco Zone, during this fiscal year, 6 pieces of representative rock samples were collected in order to measure their resistivity and FE values in the laboratory. Table II-2-1 indicates the results obtained in this survey as well as the ones obtained during the Phase I Survey (CSAMT survey).

Table Ⅱ −2−1 Resistivity and FE of Rock Samples in Osohuayco,Balzapamba Area

	Sample No.	Rock Name	Occurrence	ρ (Ω · m)	FE (%)
1	C 2074	holnfels	py film	4,560	23.7
2	C 2075	holnfels	qtz-py network	1,060	1.3
3	C 2076	holnfels	silicification	13,070	0.3
4	C 2077	leucocratic granite		11,100	0.2
5	B 2087	granodiorite	py disssemination	7,080	4.3
6	B 2104	granodiorite	altered	2,850	1.0
	CSAMT 24	fine-grained granodio.	silicification	6,390	4.0
	CSAMT 33	qtz bearing and. tuff	silicification	15,000	2.1
	CSAMT 36	qtz bearing and. tuff		2,760	2.3
	CSAMT 401	granodiorite		7,720	3.2
	CSAMT 405	granodiorite	silicification	16,150	3.6
	CSAMT 413	grossular-qtz vein		2,660	0.5

According to these results, resistivity of granitic rock samples range from 2,850 to 16,150 Ohm-m while resistivity of Macuchi formation samples range from 1,061 to 15,000 Ohm-m. No definitive difference can be found between both type of rocks, since the resistivity changes during the alteration process are considered to be even greater than their deferences between both types. Therefore, the resistivity changes detected during the present survey indicate mainly changes in the alteration process rather than changes in rock type, reflecting in such a way, low resistivity for argillization and high resistivity for silicification.

On the other hand, disseminated sulphide are widely seen in this area, with stronger indication in granitic rocks than in Macuchi formation. As a result, high FE anomalies obtained during this survey correspond to granitic rocks, whereas low FE anomalies to Macuchi formation.

(2) Plan maps

1) n=1 (Figs.II-2-4 and II-2-5)

a) Apparent resistivity plan map (Fig.II-2-4)

Five low-resistivity anomalies, indicated from A to E in the figure, were detected in the area, while five more anomalies were detected as high resistivity anomalies and indicated from P to T in the mentioned figure.

A general trend of resistivity changes are seen along NE-SW and ENE-WSW and reflecting actually the general trend associated to geological structures and boundaries.

Low resistivity of the anomaly A which is the biggest anomaly indicated in this map, shows a low resistivity of 155 Ohm-m at station 7 of Line 01 in its center. This anomaly shows a tendency to extend along the range and also towards ENE direction. The low resistivity values of this anomalous zone are considered to be indicative of argillization associated with mineralization.

The other low resistivity anomalies seem to reflect small scale faults, mineralization as well as alteration.

On the other hand, among the high resistivity anomalies, the anomaly P shows a rather big scale anomaly with its peak value (2,760 Ohm-m) at station 13 of line 02. This anomaly distribution seems to correspond generally to mineralization associated to a strong silicification in the third lower tuff formation.

Regarding the high resistivity anomalies Q and S, they correspond, though in an discontinuous manner, to mineralization associated with a strong silicification in the second tuff formation. Anomalies R and T give an indication of rocks of the Macuchi formation which was largely methamorphosed to hornfels or to an undefined silicified rocks.

b) FE plan map (Fig.II-2-5)

FE values utilized in this map range from -0.3% to 12.5%. Low to medium FE seems to be distributed in the southern half of the area and in northwestern end of each line, showing a medium high to high FE from stations 7 to 10 of line 03. The contour lines of 3 and 4.0% trending E-W in the center of the area, seem to correspond with the boundary of granitic rocks and Macuchi formation.

Four prominent FE anomalies of more than 4.0% are seen in the area and indicated as I, II, III and IV in the plan map.

The anomaly I, which correspond to an anomaly of more than 6.0%, is seen only in the northeastern part of the survey area, and extends towards northeast. Two anomalous peaks of 12.5% and 10.3% detected in line 01 are considered to be the superposed results of two different sources.

Anomalies of more than 4.0% were detected in the following locations:

Anomaly II: from stations 23 to 27 of line 01

Anomaly III: from stations 7 to 9 of line 03 as an extension of the anomaly I from stations 3 to 7 of line 06

Anomaly IV: from stations 3 to 7 of line 06

2) n=3 (Figs.II-2-6 and II-2-7)

The center of each anomaly seems displaced with respect to the corresponding location detected for n=1 anomalies. This effect seems to be due to the typical pants-leg pattern conformed by the dipole-dipole array used in this survey and which make them to be interpreted as another anomaly.

a) Apparent resistivity plan map (Fig.II-2-6)

This pattern resembles that of n=1 of Fig.II-2-4, but showing a tendency to increase its apparent resistivity values.

The low resistivity anomaly A gets smaller in scale than that indicated in the previous apparent resistivity plan map (n=1), and tends to merge in the anomaly B. On the other hand, the anomaly C which has a comparatively low resistivity disappears in this map, reflecting this anomaly, a rather shallow low resistivity layer.

The high resistivity anomaly Q disapears in this map, however, the remaining high resistivity anomalies seem to combine into one with bigger resistivity values.

New high resistivity anomalies are seen on the western end of the lines 01,02 and 06, indicating fresh granitic rocks.

b) FE plan map (Fig.II-2-7)

FE values utilized in this map range from 0.0 to 11.2%. As same as in its corresponding apparent resistivity map, low FE values are widely seen in the southern half of the surveyed area. Medium to high FE values are seen expanding their distribution while low FE values detected in the northwestern end from the previous map, are seen here limited their distribution to only Line 06.

High FE values of more than 8.0% are seen here from station 9 of Line 01 to station 7 of Line 03 and station 17 and its surrounding area of Line 01. The former values conform the IP anomaly I, while the latter FE values are due to a buried source seen on the section of Line 01.

The fact that the 5.0% and 6.0% contour lines of the anomaly I splits into two in the western area, suggests that this anomaly is due to the superposition of two diferent sources.

High FE values of more than 5.0% seen around station 13 of Line 06 are not seen as part of the IP anomaly III, but rather conforming the pants-leg pattern of anomaly IV.

3) n=5 (Figs.II-2-8 and II-2-9)

a) Apparent resistivity plan map (Fig.II-2-8)

As compared with n=3 plan map indicated in Fig.II-2-6, the apparent resistivity distribution pattern for n=5 is seen rather simplified and showing higher resistivity values.

The low resistivity values of 122 Ohm-m observed in this map seems to be actually due to the superposition of two low apparent resistivity anomalies A and B, both showing the typical pants-legs pattern. A diferent low resistivity anomaly F is seen in the southeast of the above mentioned anomaly. However, the low resistivity anomaly D is no longer seen in this map, but appears instead as a relatively low resistivity zone.

High resistivity anomalies P2 and T in previous map are seen here combined into one forming the anomaly W, whereas the high resistivity anomalies P1 and S are kept the same as before, however the high resistivity anomalies R and U experience higher values. High resistivity anomaly V also vanishes, but shows a high resistivity zone in the northwest of Lines 05 and 06.

b) FE plan map (Fig.II-2-9)

The FE values used in this map varied from -2.5% to 13.5%.

5.0% contour line of anomaly I is seen extended forming a tongue shape pattern up to the center of line 05 connecting with anomaly IV.

A medium high FE anomaly of 6.0% is detected at station II of Line 06, which is considered to be due to the superposition effects of the two pants-leg pattern anomalies

III and IV.

(3) IP pseudo-sections

1) Line 01 (Fig.II-2-10)

A strong variation in both apparent resistivity and FE values are seen on this line, with resistivity values ranging from 122 to 5,060 Ohm-m and FE values from -2.5 to 22.0%.

A low resistivity distribution was detected from a shallow zone at stations 4 to 10 to the depths of station 11. A high FE anomaly is also detected conforming a pants-leg pattern with station 6 as its center. This result corresponds to the low resistivity anomaly A and IP anomaly I mentioned in the plan map description. This low resistivity/high FE overburden is assumed at around stations 4 to 10. At the depths of this area, a high resistive body with medium to high FE distribution (anomaly U), suggests a structure due to silicification associated with mineralization at the shallow part.

A medium resistivity and high FE is detected as a part of anomaly I in the shallow part of stations 10 to 14.

Low resistivity and medium FE seen in the southeastern part of this area seems to be due to mineralization along the fault.

In the area around station 20, a part of the pants-leg pattern anomaly of low resistivity (anomaly C) and low FE suggests either faults or a geological boundary. At the depths and to the northwestern part of this boundary, a high FE (IP anomaly V) is observed, while in its southeastern side a low FE is detected.

High FE and low resistivity (anomaly F) found in the north western side of the area reflects a probable buried mineralization.

A rather weak pants-leg pattern anomaly (IP anomaly II) is seen around station 25 where mineralization is likely to exist.

2) Line 02 (Fig.II-2-11)

On this line apparent resistivity varies from 623 to 3,950 Ohm-m and FE values from 2.0 to 9.7%. Both fluctuations are moderate.

High FE anomaly corresponding to IP anomaly I is detected at middle depth in station 10 and decreasing its FE values towards northeast and southeast.

A resistivity body is assumed at middle depth of stations 14 to 20 (anomalies P and W) and at the depths of stations 24 to 30 (anomaly R). Around stations 21 to 25 it is seen an indistinctive high resistivity body at shallow depths (anomaly Q), whereas an indistinctive low resistivity is seen at the depths (anomaly C). On the other hand, their high FE distribution of more than 9.0% seems to be relatively higher than in the surrounding area, suggesting the existence of a weak silicification associated with

mineralization in the same formation.

3) Line 03 (Fig.II-2-12)

Apparent resistivity values range from 440 to 3,160 Ohm-m.

High resistivity of more than 2,500 Ohm-m detected at middle depths of stations 9 to 13 (anomaly P1) and at the depth of stations 16 to 25 (anomaly W) suggest the existence of a resistive body in the corresponding depth.

FE values range from 1.2 to 10.0%, and medium to high FE anomaly corresponding to anomaly I were detected in the north western half of the line.

IP anomaly I is conformed by two pants-leg pattern anomalies with their peaks at stations 9 and 11 respectively. A 10.0% FE peak seems to be superposed by both anomalies in the north western part.

IP anomaly I distribution is thought to be due to a high resistive at the depths of station 10 where silification associated with mineralization is assumed.

4) Line 04 (Fig.II-2-13)

Low to medium resistivity values are seen only between stations 12 and 26 and around the north western part of this line. However, high resistivity values from 468 to 5,960 Ohm-m are also predominant, and this high resistivity delineated by the contour line of 2,500 Ohm-m suggests the presence of high resistivity rocks at depths.

On this line, FE values range from 1.0 to 6.0%. Medium to high FE values, which correspond to IP anomaly I, are detected in the area between stations 4 and 15. This anomaly is seen in the IP pseudosection as formed by two pants-leg pattern anomalies with their corresponding centers at station 7 and 11 respectively. The pants-leg pattern under station 11 can be interpreted as the result of a source of anomaly at a moderate depth.

On this section, this IP anomaly I, at depths of station 10, seems to be caused by silicification associated with mineralization and conforming a resistive rock at its center.

5) Line 05 (Fig.II-2-14)

Apparent resistivity values range from 475 to 4,300 Ohm-m, showing a more complicated pattern than the previous pseudosections 02, 03 and 04. This complexity may be due to several small scale conductive overburdens on this line.

From station 24 towards southeast a high apparent resistivity of more than 2,500 Ohm-m suggests a resistive body at depths.

FE values range from 1.4 to 5.7%, indicating anomalies at stations 8, 11 and 17. The IP anomaly detected at station 17 is considered to be the extension of the IP anomaly seen

at station 11 of the previous line (line 04)

6) Line 06 (Fig.II-2-15)

The apparent resistivity values, which range from 327 to 1,740 Ohm-m, are comparatively lower than those of the previous lines. This low apparent resistivity is actually due to a thick conductive overburden in this area, especially in the central part of this line where a quite different resistivity structure is suggested.

FE values range from -0.7 to 6.8%, showing IP anomalies at stations 6 and 16. These anomalies correspond with the anomalies III and IV described above and which are considered to be due to silicification associated with mineralization. Little correlation is seen with the other IP anomalies detected on the other sections.

(4) Simulation analysis

Simulation studies were carried out for the Lines 01, 03 and 04 of the Osohuayco zone. The simulations covered an extension between the stations 0 and 20. Some of them, assumed resistivity structures up to station 24. However, reliability of geometries and values simulated between stations 20 and 24 are considered lower than that between stations 0 and 20.

1) Line 01 (Fig.II-2-16)

As a result of the general trend in the IP survey in this line, it can be summarized as having a high resistivity and medium to high FE around stations 4 to 14 and medium resistivity and low FE in the south of station 14.

Background values in the north of station 4 result in 4,000 Ohm-m in resistivity and 3.0% in FE, and corresponding to fresh granitic rocks. At stations 2 to 4, values on the surface, show 1,500 Ohm-m and FE 2.0%, which are assumed as the results of a weathered layer.

Comparatively low resistivity of less than 700 Ohm-m represents the background value at stations 4 to 14. However, high FE values of more than 8.0% were detected in the area excluding at medium depth of stations 6 to 9. This can be interpreted as an argillization zone associated with mineralization.

The superficial layer at stations 4 to 12 are especially assumed to be of a rather low resistivity (80 to 350 Ohm-m) and to be due to a strong argillization process.

Medium resistivity of 1,000 to 1,500 Ohm-m, which is assumed for the areas between stations 9 and 11 and between 12 and 14, reflects a rather weak silicification.

At the depth of station 10, it is assumed that a north dipping dyke-shape body, with 4,000 Ohm-m in resistivity and 10.0% FE, is influenced by strong silicification associated

with mineralization.

Background values in the south of station 14 result in 2,000 Ohm-m in resistivity and 3.5% in FE corresponding to a weakly altered granite. Low resistivity zone on the surface of stations 20 to 24 correspond to argillized Macuchi formation showing strong mineralization at stations 20 to 22.

From the surface to the depths at stations 14 to 16 and at the depth of stations 20 to 22, a dyke-shape body is assumed, which has a resistivity of 2,000 to 3,500 Ohm-m and FE of 10.0 to 12.0%. These values seem to be the results of a strong silicification associated with mineralization.

2) line 03 (Fig.II-2-17)

As a general trend detected in this line, it is safe to say that the north of station 6 (Block No.2) indicates low resistivity, south of station 8 (Block No.11) shows middle resistivity and the area between both blocks shows high resistivity. In these areas, the background of FE values detected ranges from 2.0 to 3.5%, being the lowest FE located in the south of station 18.

In the north of station 6, the background values are estimated in 500 Ohm-m in resistivity and 3.0% in FE, corresponding these values to granitic rock strongly weathered and affected by argillization. From the simulation results, it is inferred that the superficial layer between stations 6 through 8 (Block No.10) and its deeper information (Block No.13) had been strongly affected by silicifation associated with mineralization. Resistivity values in this area ranges from 2,700 to 3,500 Ohm-m, while interpreted FE values ranges from 4.0% on the surface to 13.0% at the depths, suggesting deep silicification associated with mineralization.

In the area, between stations 8 and 14, the background values which amount to 2,000 Ohm-m in resistivity and 3.5% in FE (Block No.1), correspond to weakly altered granite.

At the depths of station 10 (Block No.15) it is suggested a south dipping structure of 4,000 Ohm-m in resistivity and 12.0% in FE, which turns out to be due to a strong silicifation associated with mineralization. On the shallow part of this area (Blocks No. 6 and 7), a structure in block is suggested with middle resistivities ranging from 1,200 to 1,500 Ohm-m and a medium-high FE from 6.0 to 7.0%. This structure is interpreted as due to weak argillization associated with mineralization.

In the south of station 14, the background values of FE are low (2.0 to 3.0%) and corresponding with Macuchi formation. The shallow layer around stations 14 to 20, with resistivity values from 700 to 1,200 Ohm-m (Block Nos. 3, 4, and 5), seem to be weakly argillized.

A south dipping structure with resistivity of 3,500 Ohm-m and FE of 6.0% assumed in

the area between stations 14 and 17 (Block No.17) is interpreted as being due to silicification associated with mineralization.

3) Line 04 (Fig.II-2-18)

In the north of station 2, a low resistivity of 300 Ohm-m and low FE of 1.0% (Block No.2) corresponds to strong altered and weathered granitic rocks. In the south of this station, interpreted results gave middle resistivity values from 1,000 to 2,000 Ohm-m and low FE from 1.5 to 4.5%.

In the north of station 10 (Block Nos. 5, 8, 1 and 14), interpreted results correspond to granitic rocks affected by alteration and weathering, however, the south of this station (Block Nos.6, 17, 7 and 10) as compared with the north side, shows lower values of resistivity (500 to 1,300 Ohm-m) and FE (1.5 to 2.5%) corresponding to Macuchi formation.

At the depths of station 0 to 12, a high resistive (2,500 to 4,500 Ohm-m) and high FE (5.0 to 10.0%) anomaly is interpreted as consisted of four bodies due to silicification associated with mineralization. Among them, a south dipping structure (Block No.12) at the depths of stations 10 to 12 has a interpreted resistivity of 4,500 Ohm-m and FE of 10.0%, suggesting from this result, that in this line the most strongly silicified and mineralized body is being present.

A two-layered structure was interpreted at the depths of station 12 having a resistivity of 1,800 Ohm-m and a FE of 2.0% in the upper layer and 2,000 Ohm-m and 4.0% in the lower layer. The former layer reflects Macuchi formation, while the latter indicates altered andesitic rocks. At the depths of station 18, a south dipping structure (Block No.11) with resistivity of 2,500 Ohm-m and FE of 8.0% has been interpreted to be due to silicification.

Finally, regarding the resistivity and FE values used for the simulations in the basement, a resistivity from 4,000 to 5,000 Ohm-m and a FE of 4.5% were assumed at the depth of 300m from the surface and for the 3 lines. These values, which need not to be well defined for the modeling, were assumed by taking into account the values determined from the electrical measurements in the rocks samples.

2-2-5 Discussion

The main mineralization in this area seems to have a good correspondence with the high resistivity and high FE anomalies caused by the strong silicification associated with mineralization.

Assuming the above mentioned resistive/high FE body as the source of the IP anomaly,

and taking into account the results of the model simulation carried out on the lines 01, 03 and 04, the location of anomalous sources under the other three lines have been qualitatively selected. These results are indicated in Fig.II-2-19, where three zones of anomalous sources trending NE-SW are indicated and named from northeast as IP anomaly sources 1, 2 and 3.

Taking into consideration the results of the geological results, the geophysical survey carried out in this zone drew the following results:

1) The geological survey revealed that mineralization is confirmed within the lower two of the three tuff formations. IP anomaly sources 2 and 3 correspond well with the above formations.

On lines 02 and 03, no indication of the IP anomaly source 3 were detected, however the trend indicated by the two anomalous sources show the same pattern than the tuff formation.

The two anomaly sources 2 and 3 are interpreted as south-dipping dike-shape body which coincides with the geological survey results.

The IP anomaly source 2 on Line 04 is interpreted as having a resistivity of 4,500 Ohm-m and FE of 10.0%, whereas IP anomaly source 3 suggests a resistivity of 2,500 Ohm-m and FE of 8.0%.

2) IP anomaly source 1 resembles somewhat the pattern of the above mentioned sources, except that this anomaly was detected in an area where granite is distributed. This source corresponds actually to mineralization found between the lines 03 and 04, in the creek between the lines 04 and 05, and in the north of Osohuayco creek.

This anomaly detected seems to be reflecting several anomalous sources because of the following reasons:

a) Dipping angle of mineralization in the north and south of Osohuayco creek are different

b) The values of resistivity, FE, width and dip do not coincide among the different lines

c) Two split anomalies were detected on Line 01

d) A fault is assumed in Osohuayco creek where mineralization is expected

3) In the center of Line 01, a wide and shallow conductive and high FE zone are interpreted, corresponding to strong argillization associated with mineralization.

To simulate the actual existence of line silicified veins, a single structure was assumed as a silicified zone existing at depth veins. This deep structure was modeled with 700 Ohm-m in resistivity and 8.0% of FE.

4) Comparing the results of the geological map with the result of FE map for n=1 clears that Macuchi formation shows a low FE while granitic rocks especially in the contact zone with Macuchi formation show high FE.

On the other hand, apparent resistivity results are considered to correlate with alteration processes rather than physical difference between geological formations: for instance, high resistivity reflects silicification; and low resistivity, argillization.

The original target in this area was to find mineralization in tuff formation, however an FE anomaly (IP anomalies I and II) of about 5.0% were detected under the tuff formation, while the most prominent IP anomaly of more than 10.0% FE was detected in granodiorite body in the northeastern part of the area.

Other IP anomalies were also detected inside the granitic rock distribution area, where they were unexpected to exist. The existence of mineralization in granitic rocks can be greatly underestimated due to poor outcropping in the area which is mainly covered by pasture. Few outcrops exist along the creek.

Regarding the IP anomaly detected under tuff formation, the measured FE resulted lower than that of northeastern anomaly, however the anomalous source determined by simulation appears to be about the same as the anomaly in granite. Consequently, the anomalous source under tuff formation was not so reflected at the surface due to the existence of a surface conductive zone, nevertheless the same scale of mineralization as in the granitic distribution area should be expected here.

In this sense, the IP method geophysical exploration used in this survey, contributed very much, especially for mineralizated zone in the less outcropped area and for the mineralized zone concealed by the Macuchi Formation. The method CSAMT carried out for the Phase I survey of this project revealed a distinctive resistivity contrast in a narrow area. The same resistivity contrast was detected also in the northern part of El Torneado area. Findings in both areas indicate prosperous mineralization. As an experience with the above results, it is recommended as a exploration methodology, to use the CSAMT method in order to detect whether or not a similar resistivity contrast exists in the prospecting area. Thereafter, in the detected anomalous area, IP method should be followed up to confirm a scale and location of mineralization precisely.

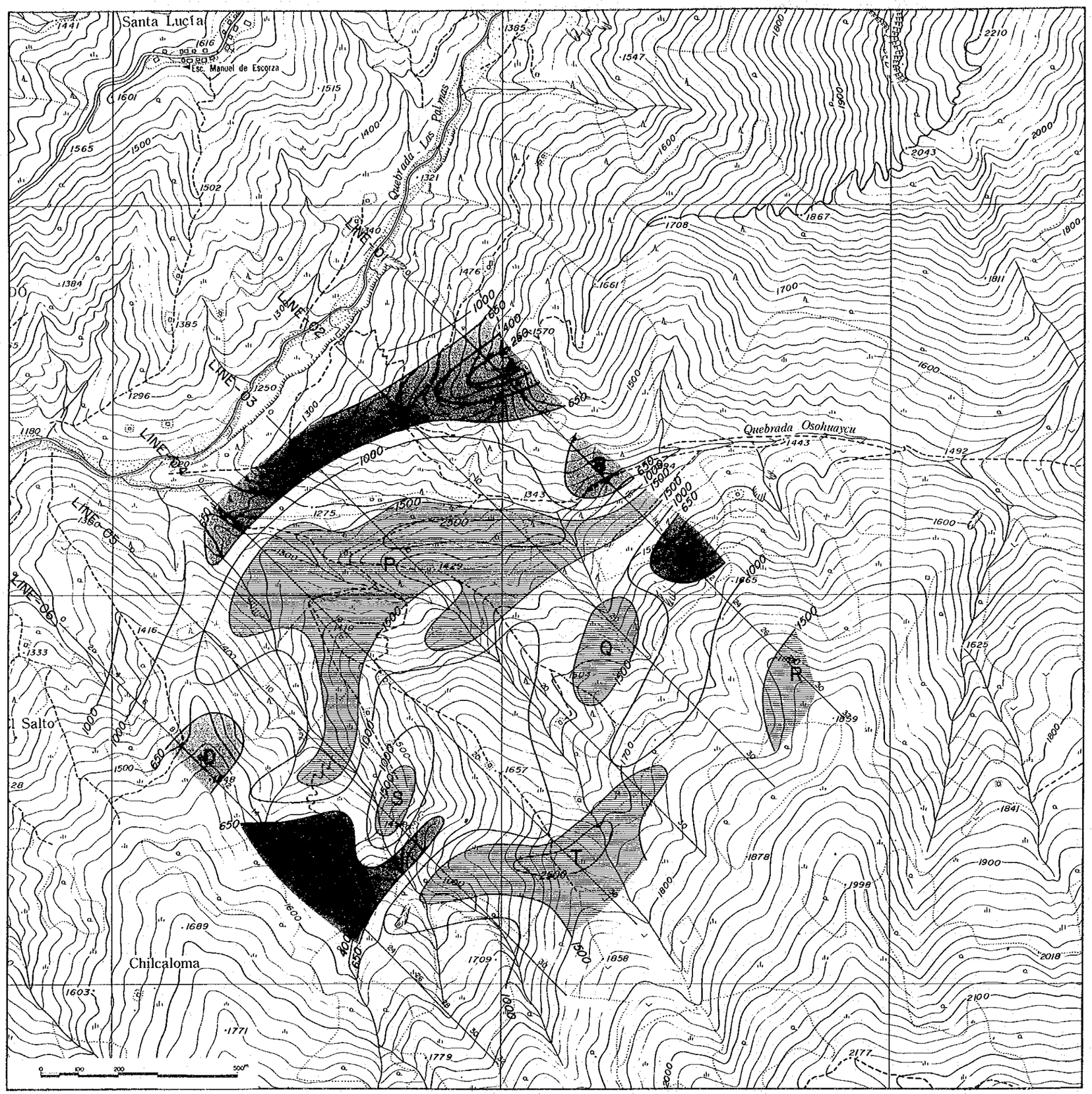

Fig. II–2–4 Apparent resistivity plan map (n=1) of the Osohuayco, Balzapamba area

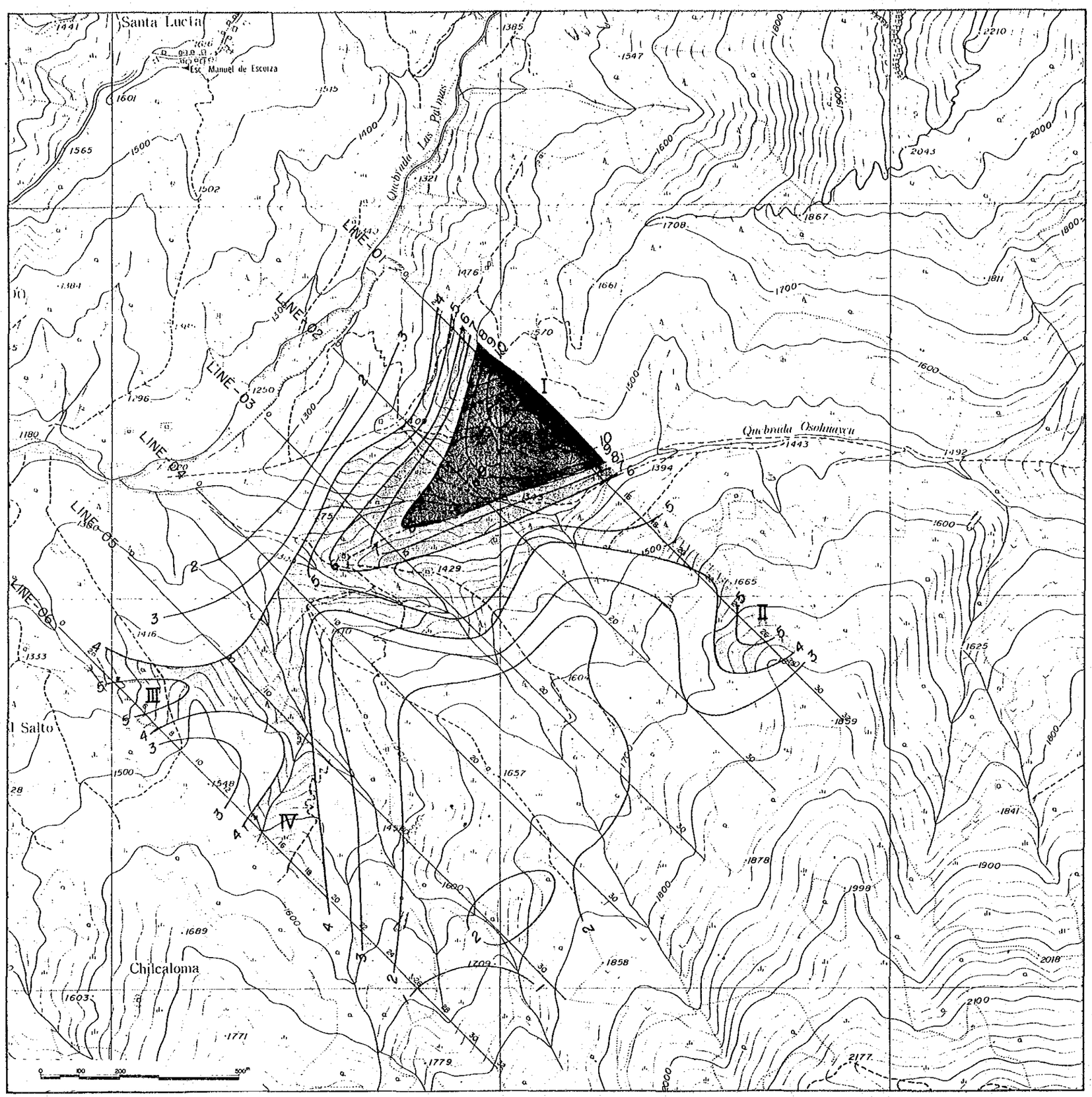

LEGEND

8.0 % ≦ p

6.0 % ≦ p <8.0 %

4.0 % ≦ p <6.0 %

p <4.0 %

UNIT : %

Fig. II–2–5 PFE plan map (n=1)
of the Osohuayco, Balzapamba area

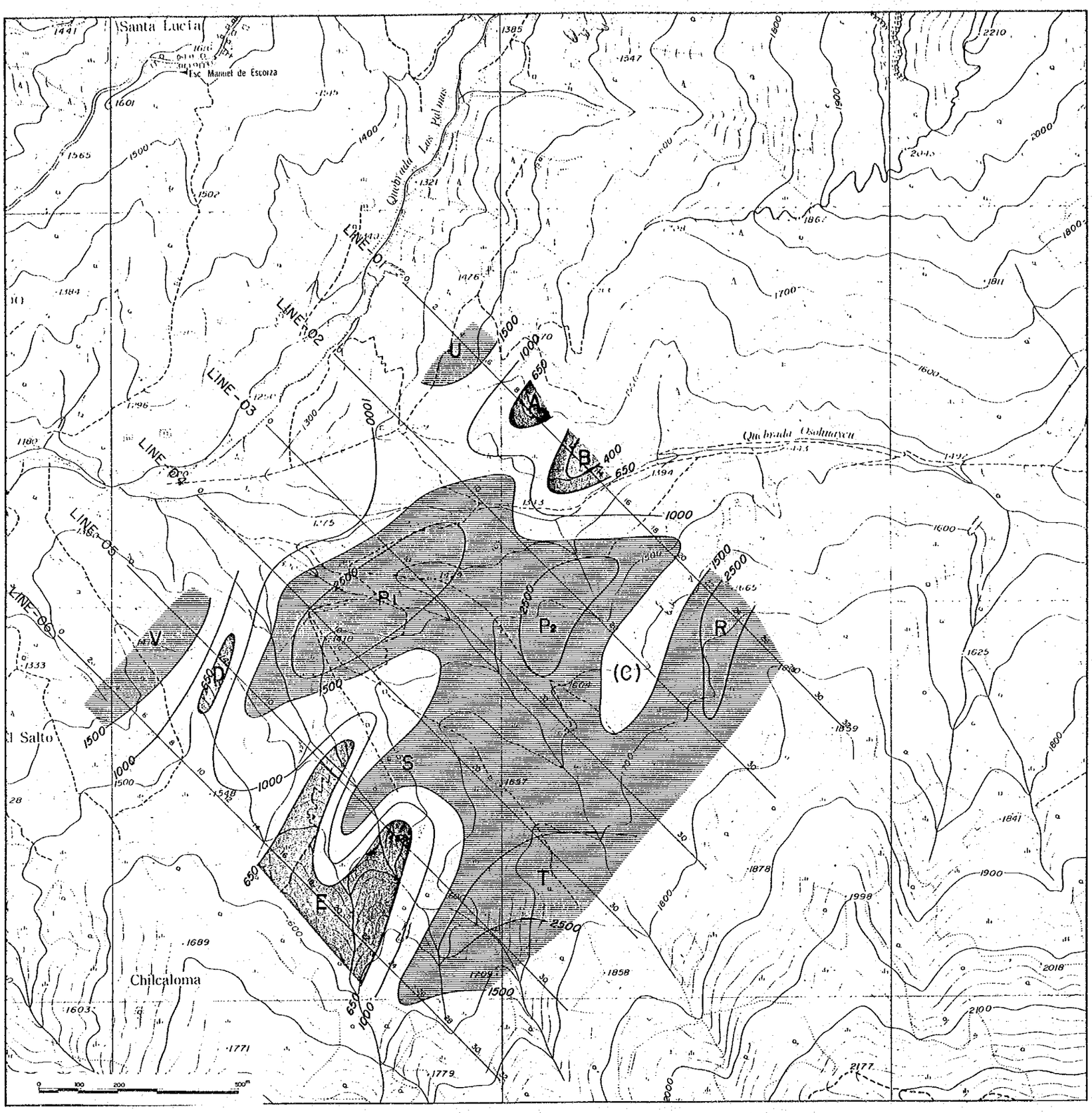

Fig. II–2–6 Apparent resistivity plan map (n=3) of the Osohuayco, Balzapamba area

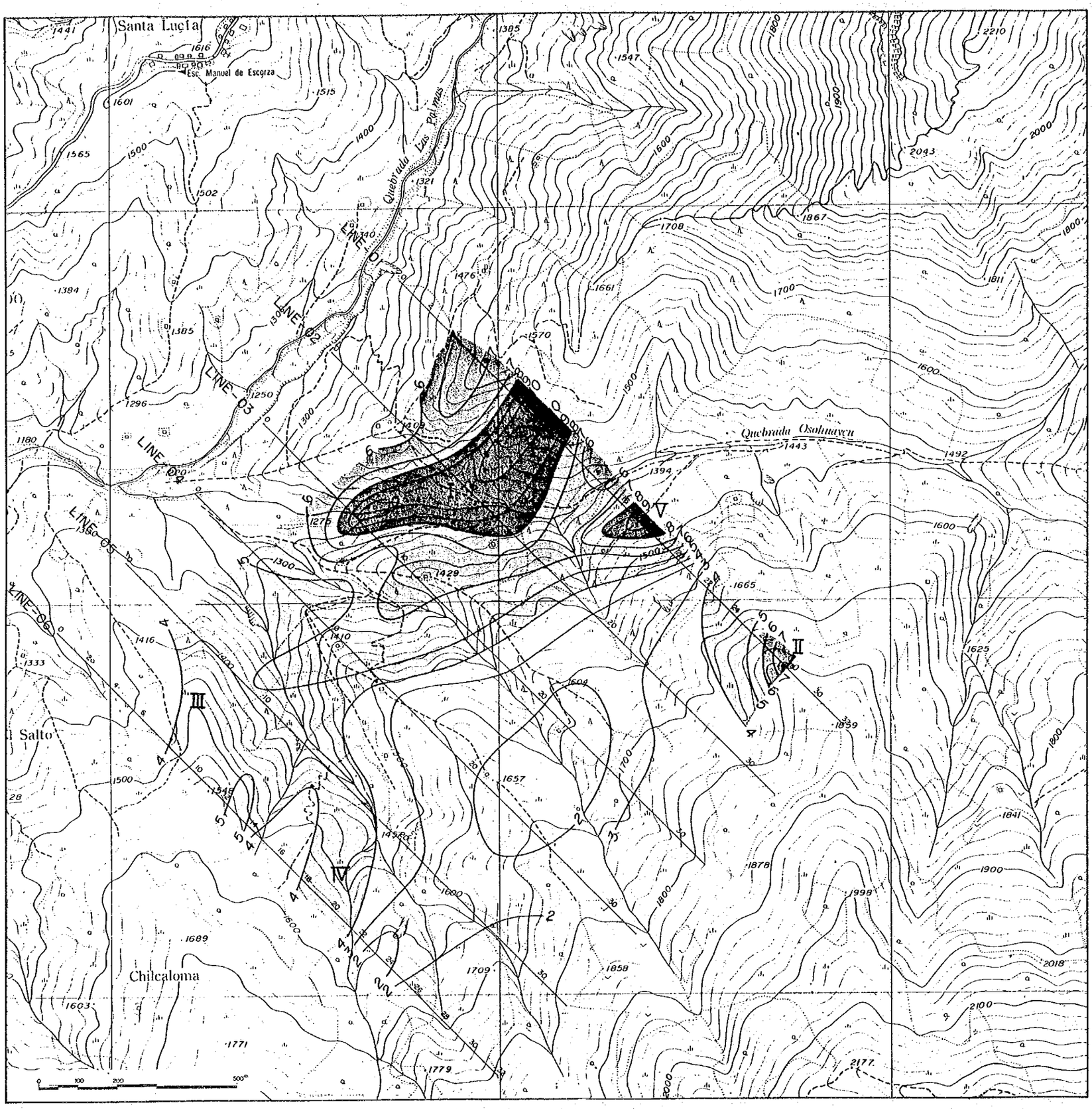

LEGEND

8.0 % ≦ p

6.0 % ≦ p < 8.0 %

4.0 % ≦ p < 6.0 %

p < 4.0 %

UNIT : %

Fig. II–2–7 PFE plan map (n=3)
of the Osohuayco, Balzapamba area

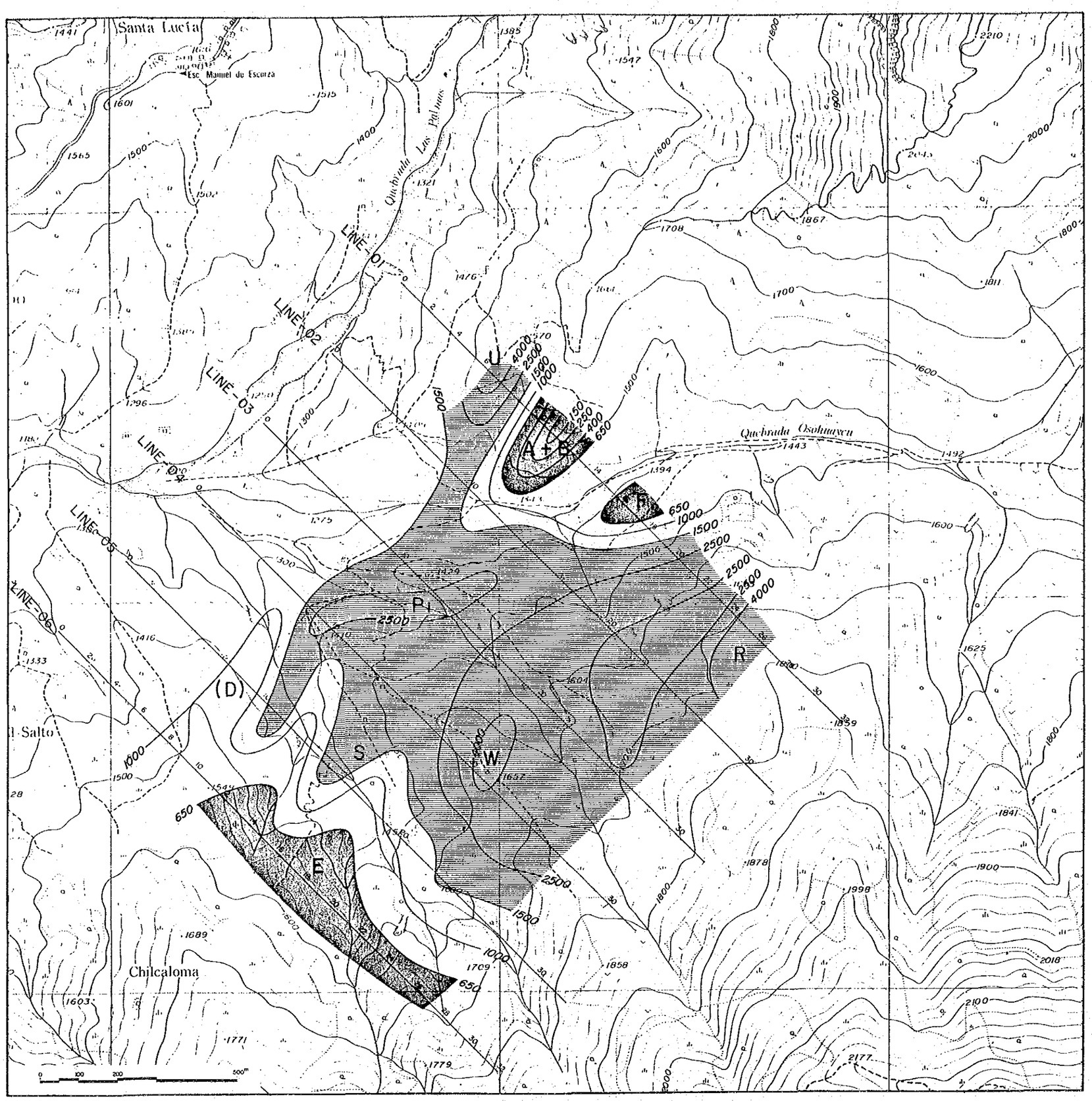

Fig. II–2–8 Apparent resistivity plan map (n=5) of the Osohuayco, Balzapamba area

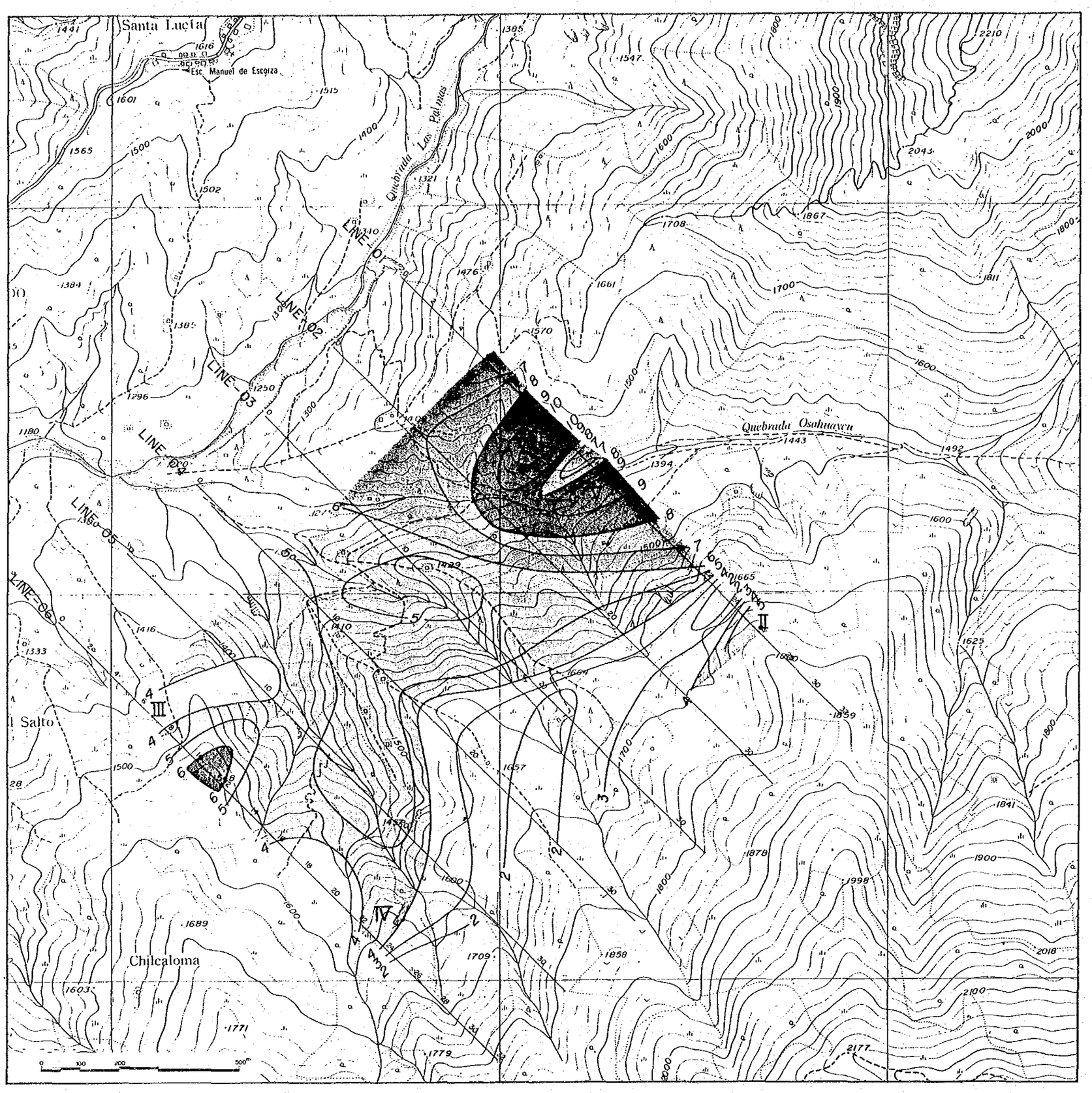

Fig. II–2–9 PFE plan map (n=5)
of the Osohuayco, Balzapamba area

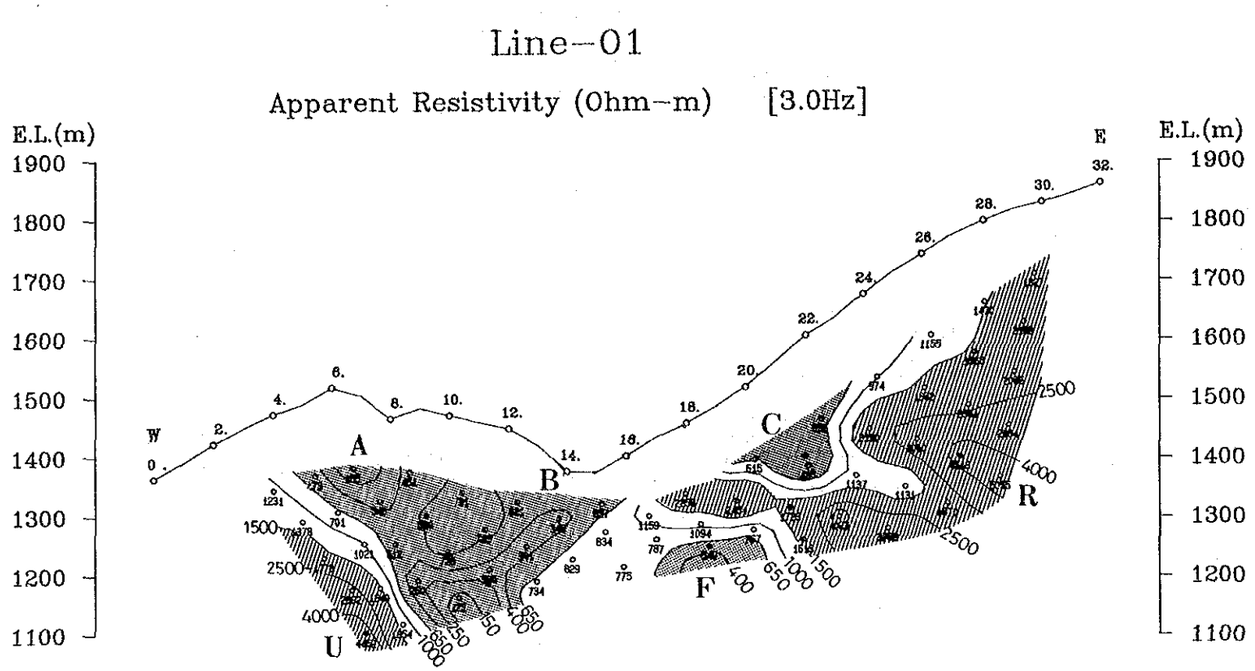

Fig. II-2-10 Pseudo-sections of apparent resistivity and PFE (line 01) of the Osohuayco, Balzapamba area

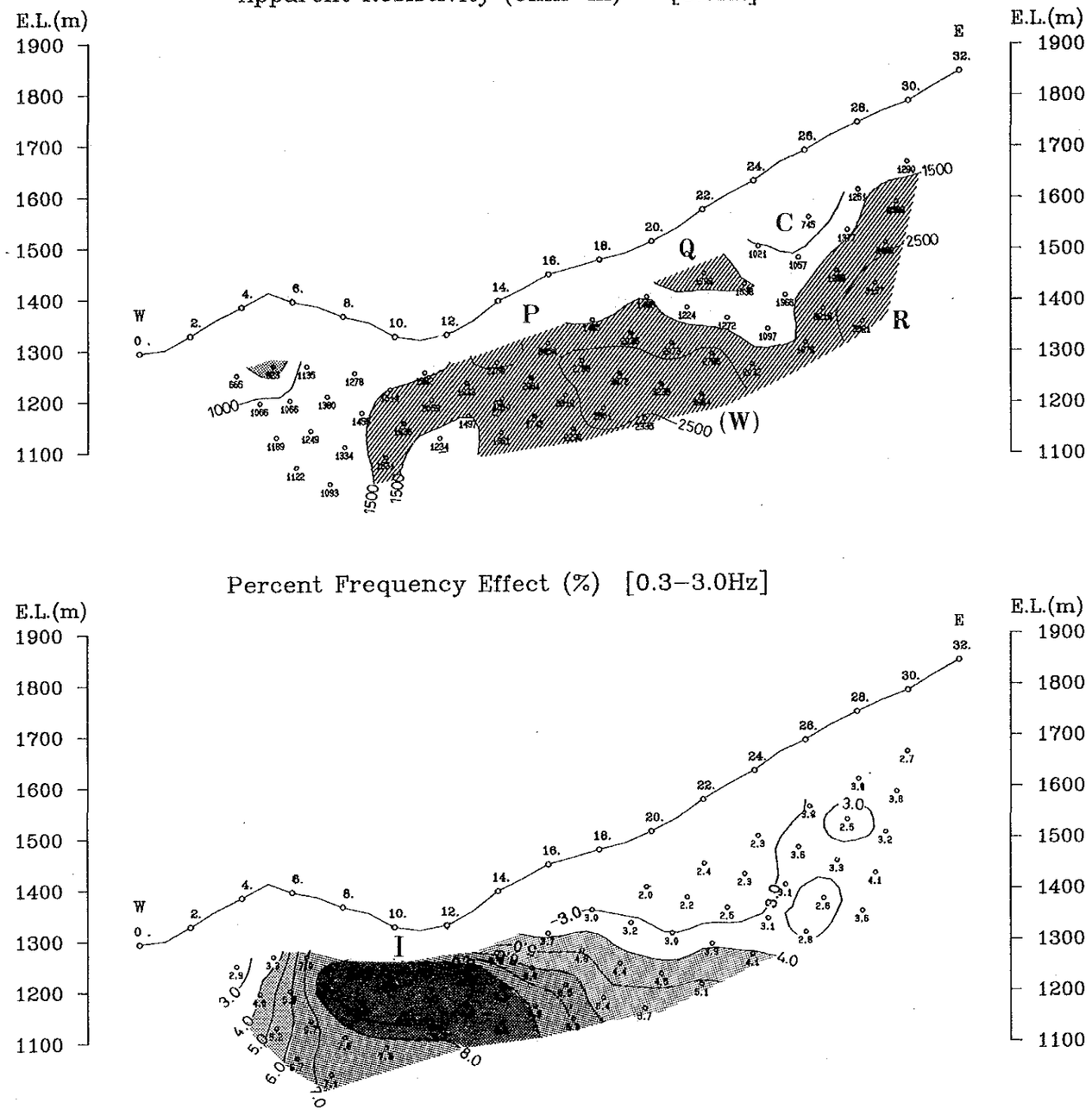

Fig. II-2-11 Pseudo-sections of apparent resistivity and PFE (line 02) of the Osohuayco, Balzapamba area

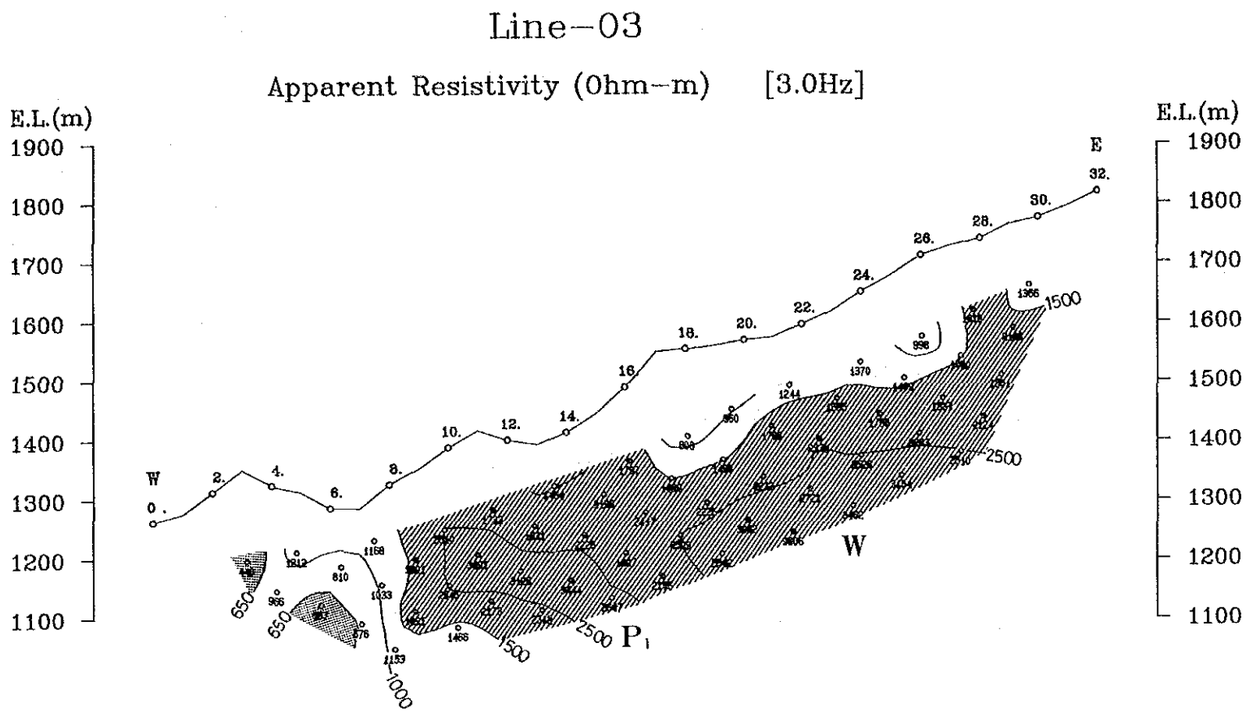

Fig. II-2-12 Pseudo-sections of apparent resistivity and PFE (line 03) of the Osohuayco, Balzapamba area

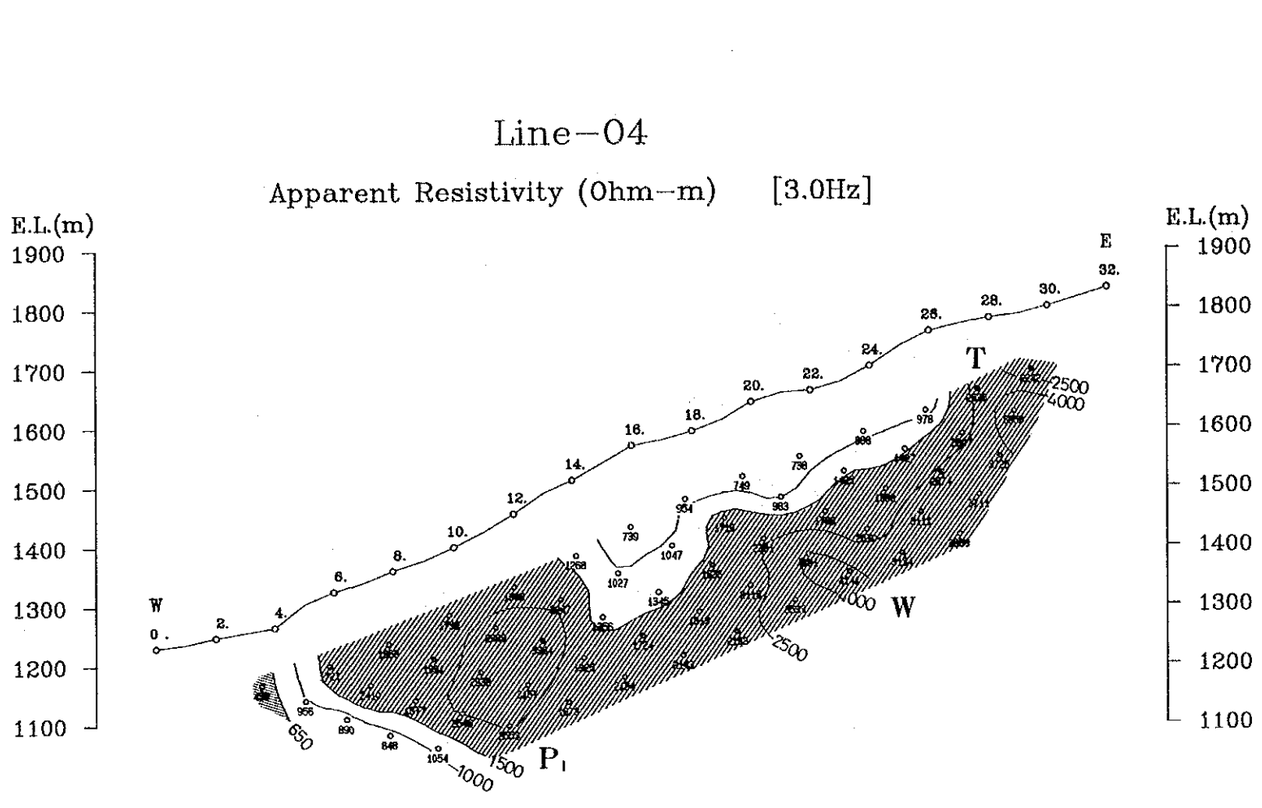

Fig. II-2-13 Pseudo-sections of apparent resistivity and PFE (line 04) of the Osohuayco, Balzapamba area

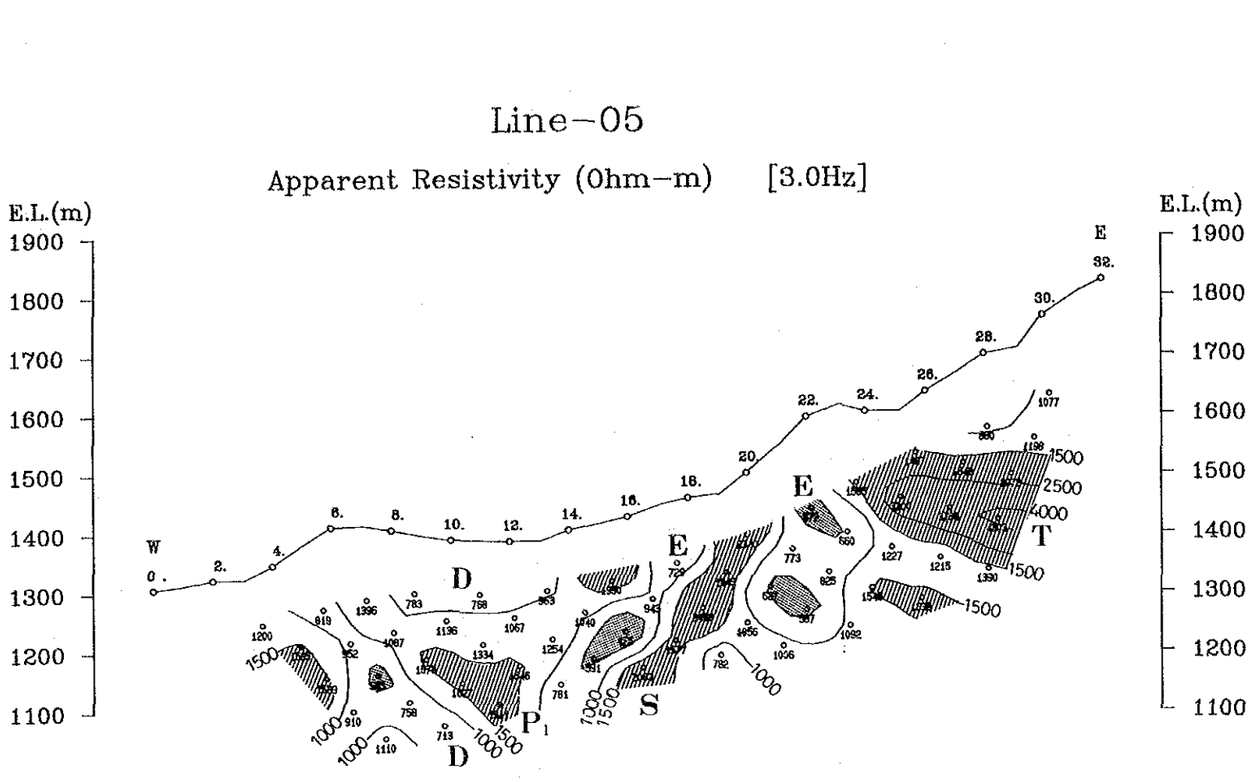

Fig. II-2-14 Pseudo-sections of apparent resistivity and PFE (line 05) of the Osohuayco, Balzapamba area

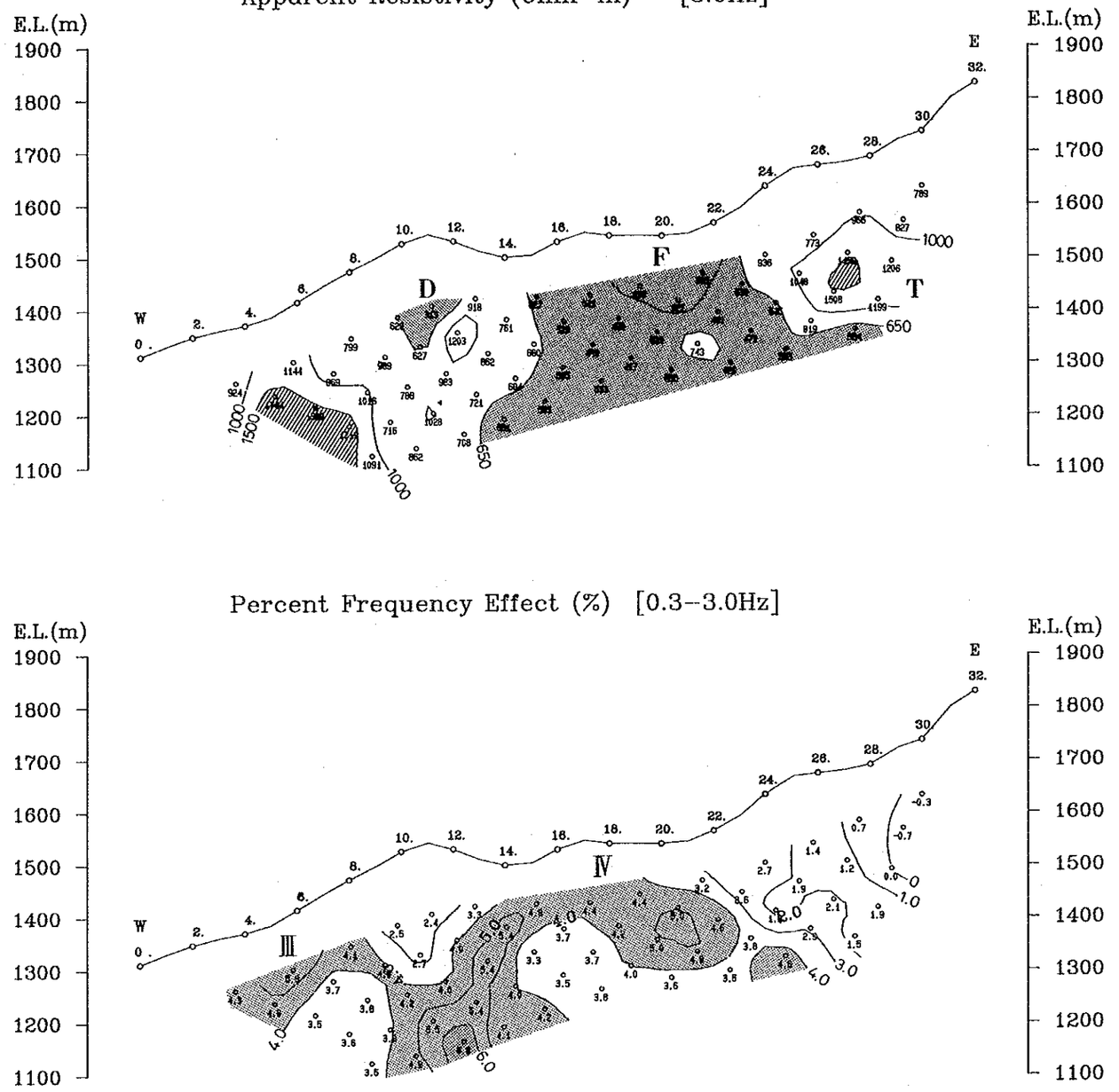

Fig. II–2–15 Pseudo-sections of apparent resistivity and PFE (line 06) of the Osohuayco, Balzapamba area

CODE NUMBER :	1	2	3	4	5	6	7	8	9	10
RESISTIVITY (ohm-m):	700.0	2000.	550.0	2000.	800.0	500.0	250.0	1500.	350.0	1000.
P.F.E. (%) :	8.00	3.50	4.00	10.0	6.00	3.00	9.00	3.00	8.50	10.0
BLOCK NUMBER :	11	12	13	14	15	16	17	18	19	20
RESISTIVITY (ohm-m):	80.00	1500.	4000.	3000.	700.0	3500.	1500.	3000.	3500.	4000.
P.F.E. (%) :	12.0	2.00	3.00	12.0	5.00	3.00	11.0	11.0	10.0	4.50

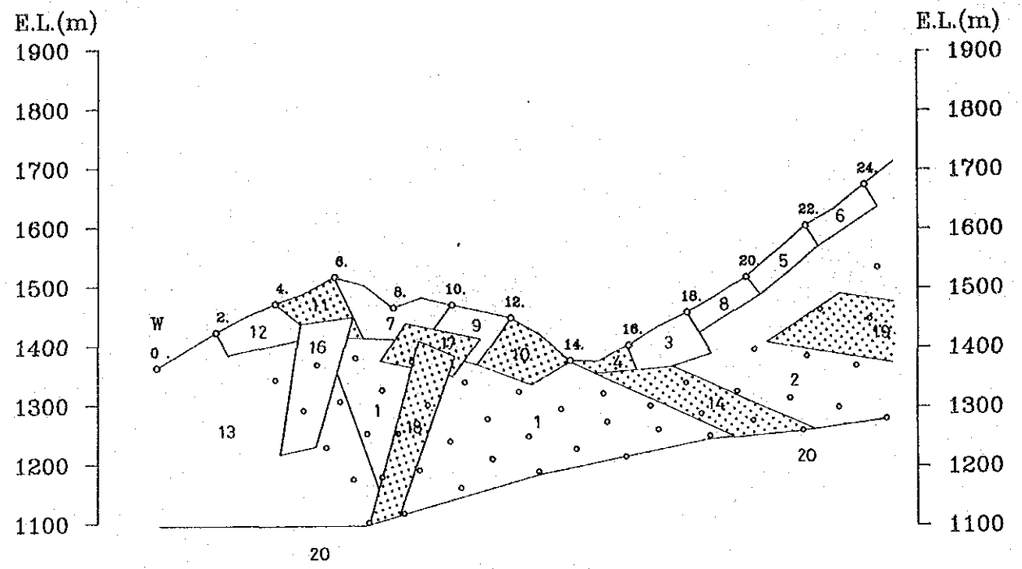

Apparent Resistivity (Ohm-m) [3.0Hz]

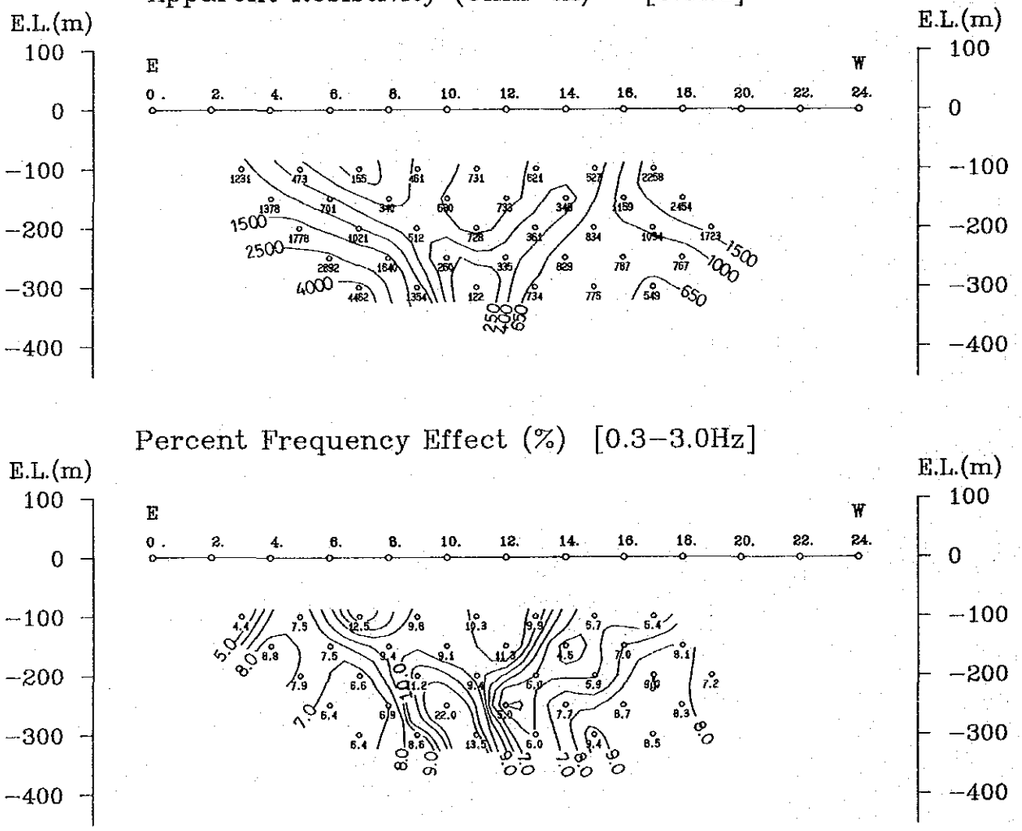

Percent Frequency Effect (%) [0.3-3.0Hz]

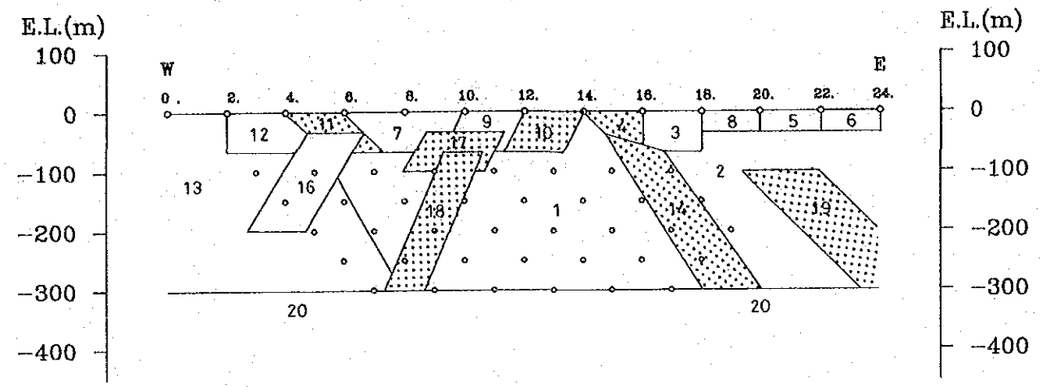

Apparent Resistivity (Ohm-m) [3.0Hz]

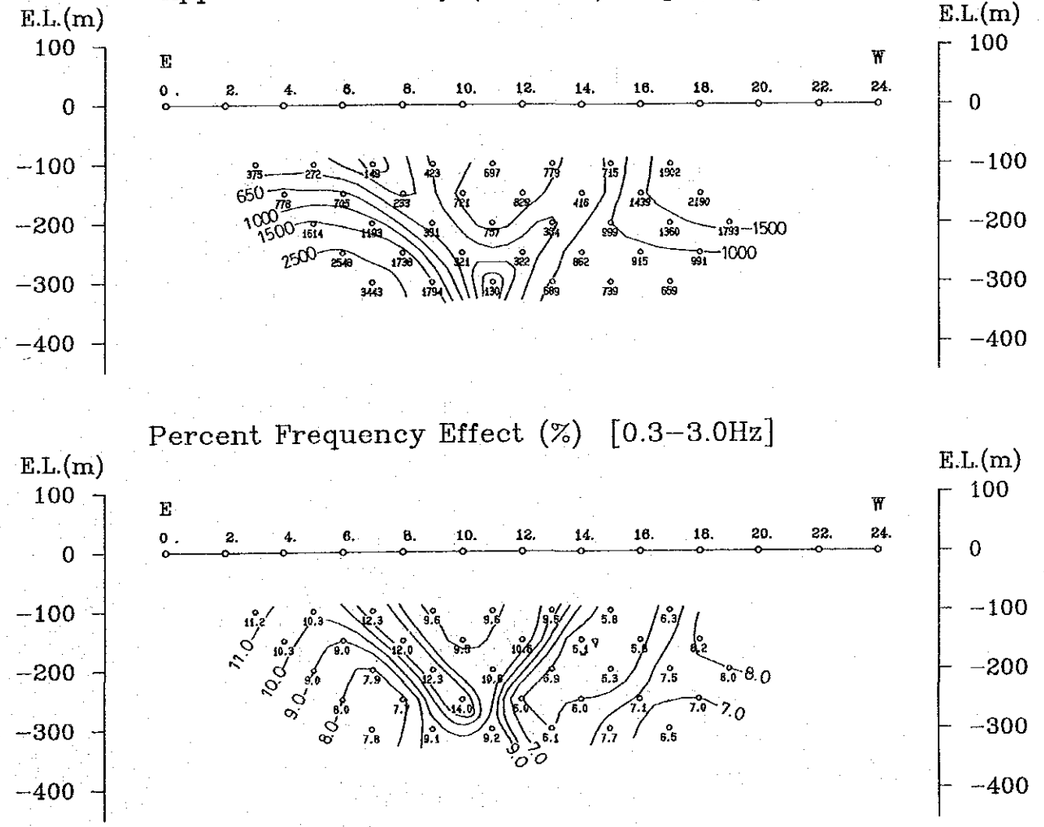

Percent Frequency Effect (%) [0.3-3.0Hz]

Fig. II-2-16 Analyzed section (line 01) of the Osohuayco, Balzapamba area

BLOCK NUMBER :	1	2	3	4	5	6	7	8	9	10
RESISTIVITY (ohm-m):	2000.	500.0	700.0	1200.	1200.	1200.	1500.	1100.	1500.	2700.
P.F.E. (%) :	3.50	3.00	2.50	3.00	3.00	6.00	7.00	4.50	2.50	4.00

BLOCK NUMBER :	11	12	13	14	15	16
RESISTIVITY (ohm-m):	2000.	1300.	3500.	3500.	4000.	5000.
P.F.E. (%) :	2.00	10.0	13.0	6.50	12.0	4.50

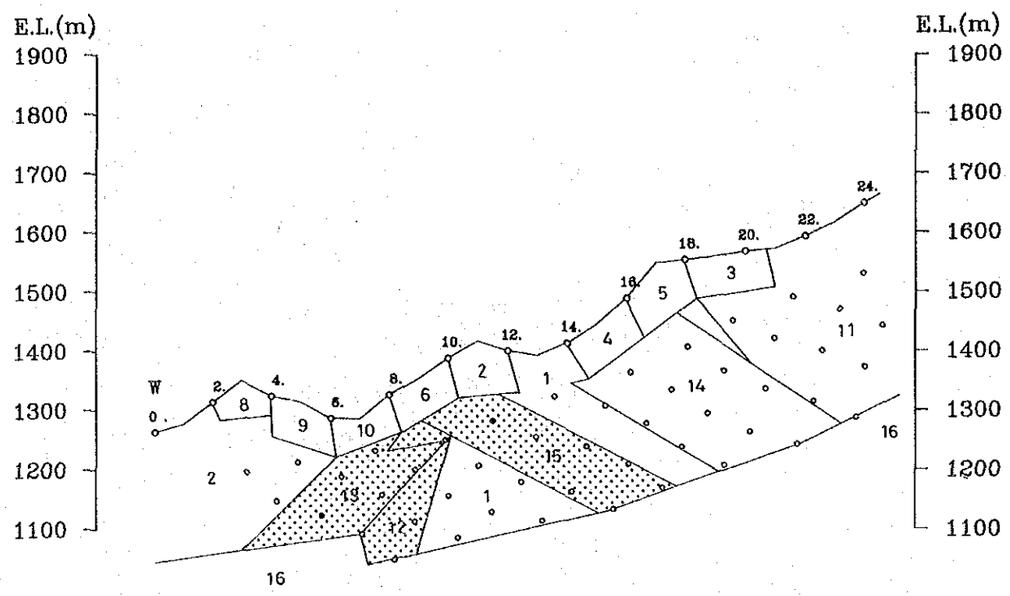

Apparent Resistivity (Ohm-m) [3.0Hz]

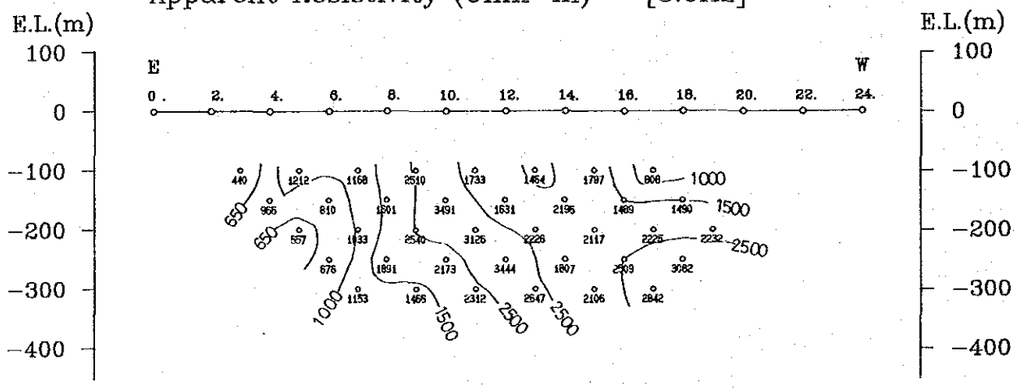

Percent Frequency Effect (%) [0.3-3.0Hz]

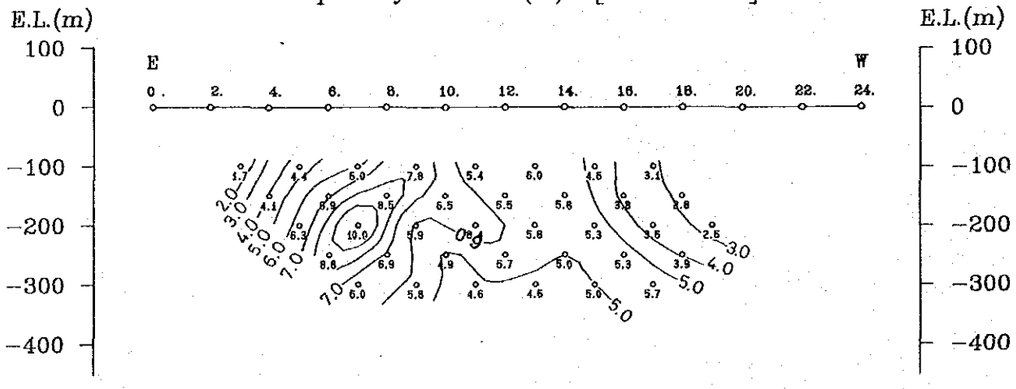

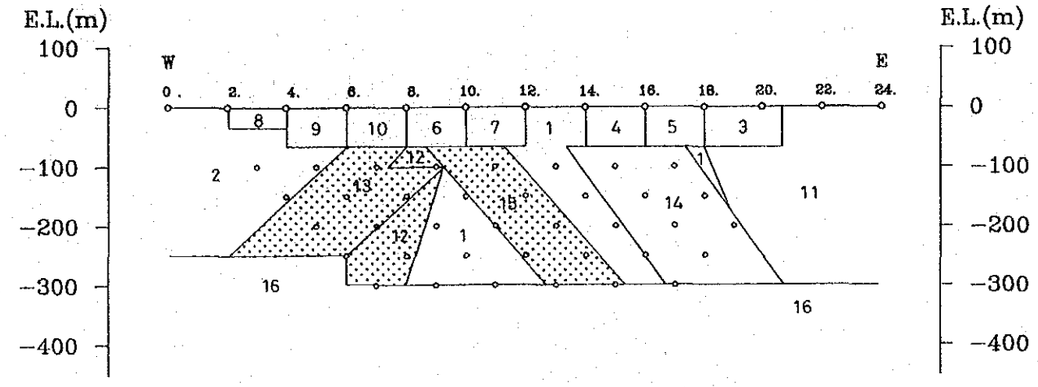

Apparent Resistivity (Ohm-m) [3.0Hz]

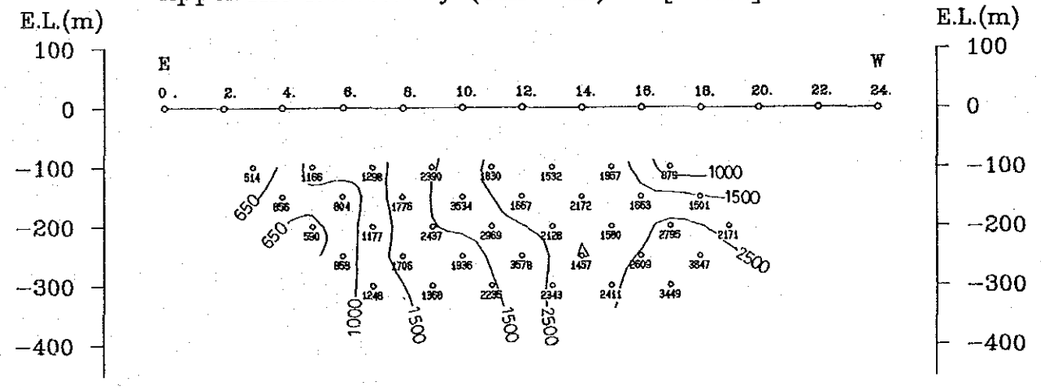

Percent Frequency Effect (%) [0.3-3.0Hz]

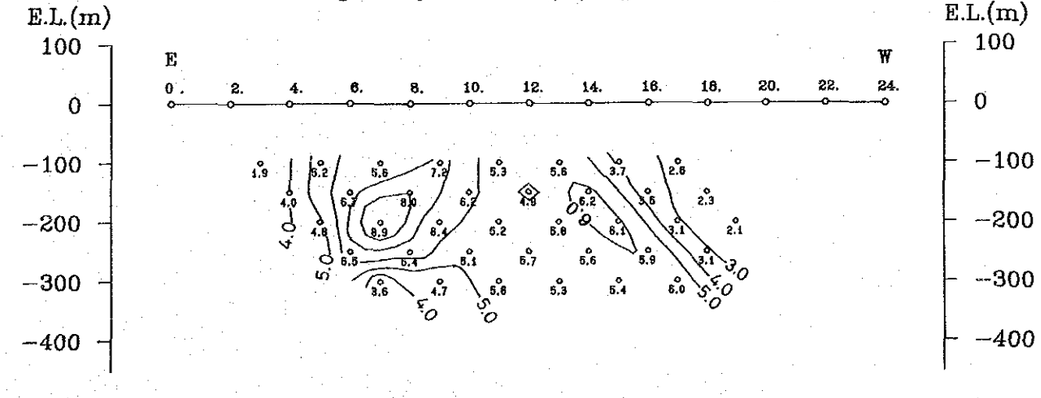

Fig. II-2-17 Analyzed section (line 03) of the Osohuayco, Balzapamba area

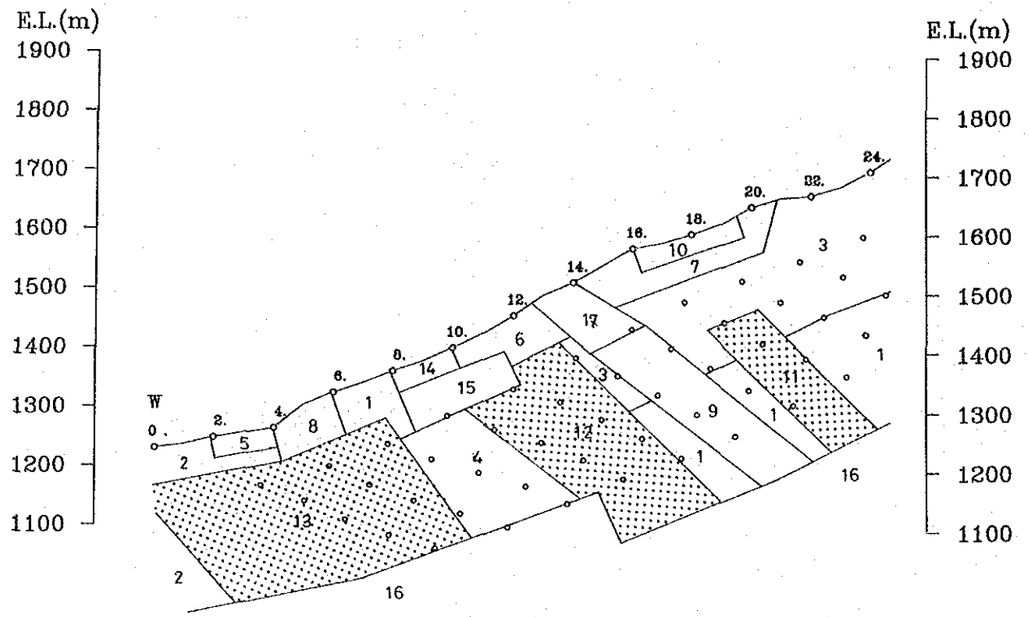

BLOCK NUMBER :	1	2	3	4	5	6	7	8	9	10
RESISTIVITY (ohm-m):	2000.	300.0	1800.	4000.	1500.	1000.	1200.	1500.	1500.	500.0
P.F.E. (%) :	4.00	1.00	2.00	6.00	3.00	2.50	1.50	3.00	3.00	2.00

BLOCK NUMBER :	11	12	13	14	15	16	17
RESISTIVITY (ohm-m):	2500.	4500.	3000.	1500.	2500.	4500.	1300.
P.F.E. (%) :	8.00	10.0	8.00	4.50	5.00	4.50	2.00

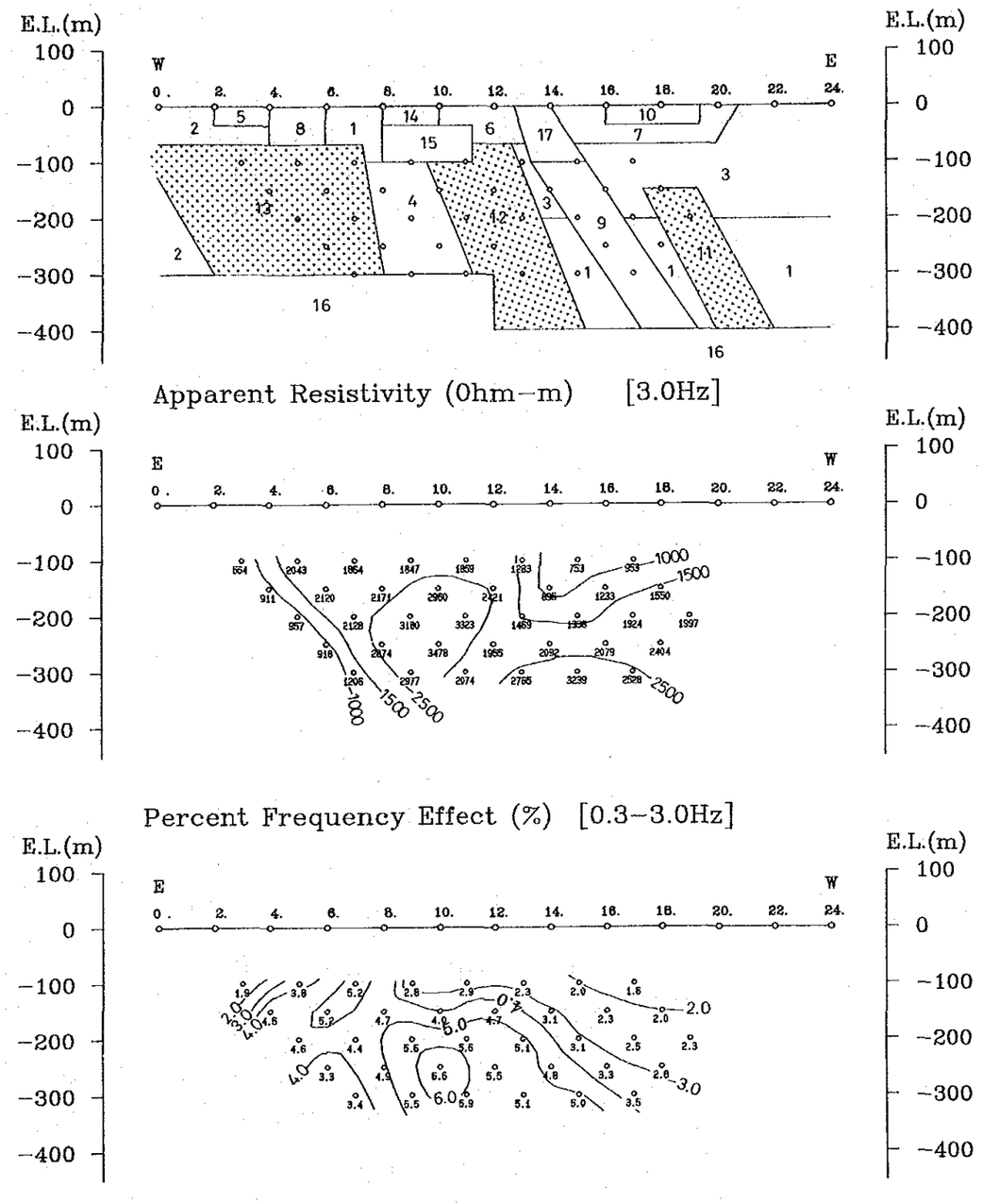

Fig. II-2-18 Analyzed section (line 04) of the Osohuayco, Balzapamba area

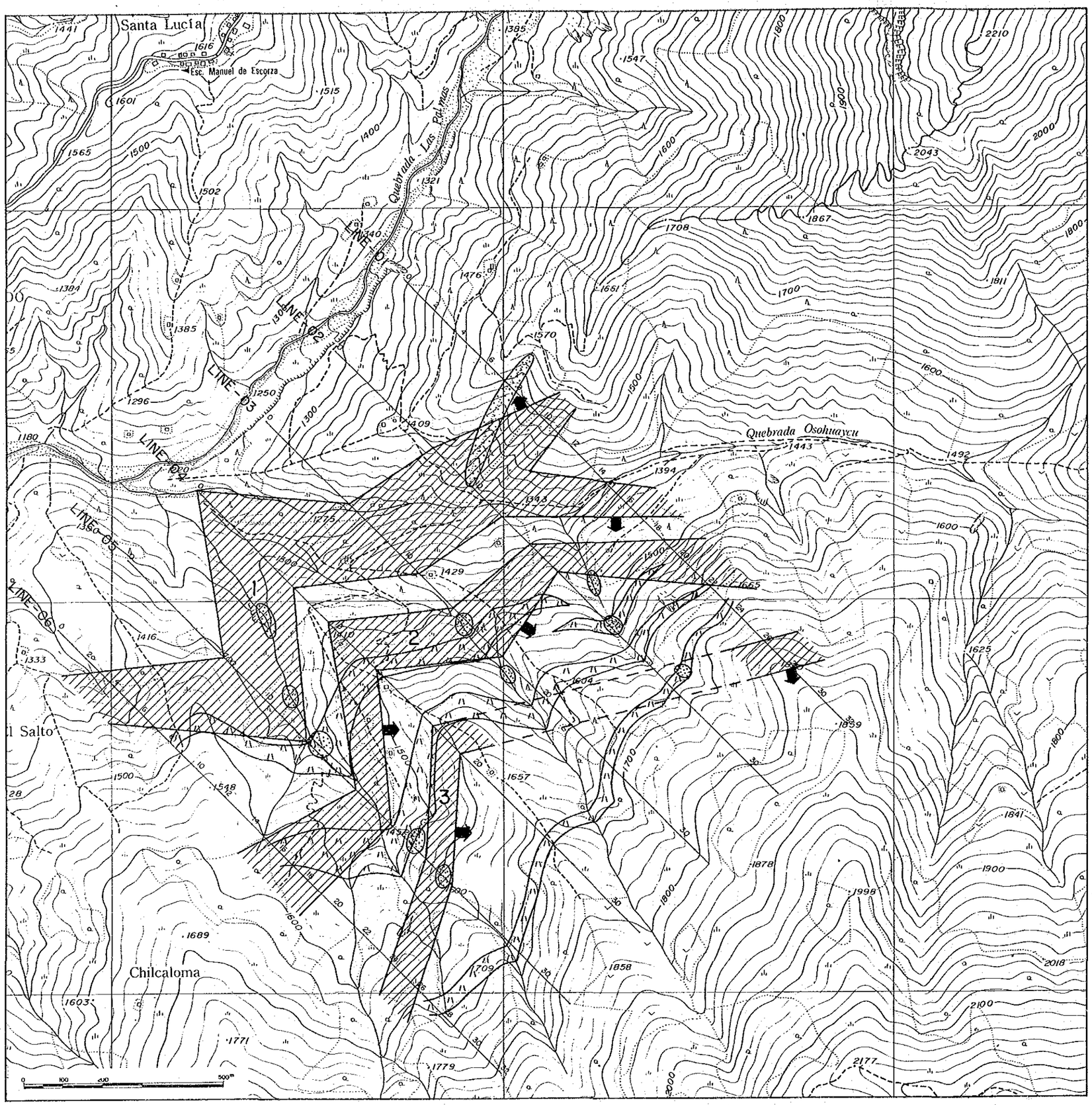

LEGEND

IP Anomaly Source (High Resistivity, High FE)

Mineralized Zone

Macuchi Tuff

Fig. II–2–19 Interpretation map of the Osohuayco, Balzapamba area

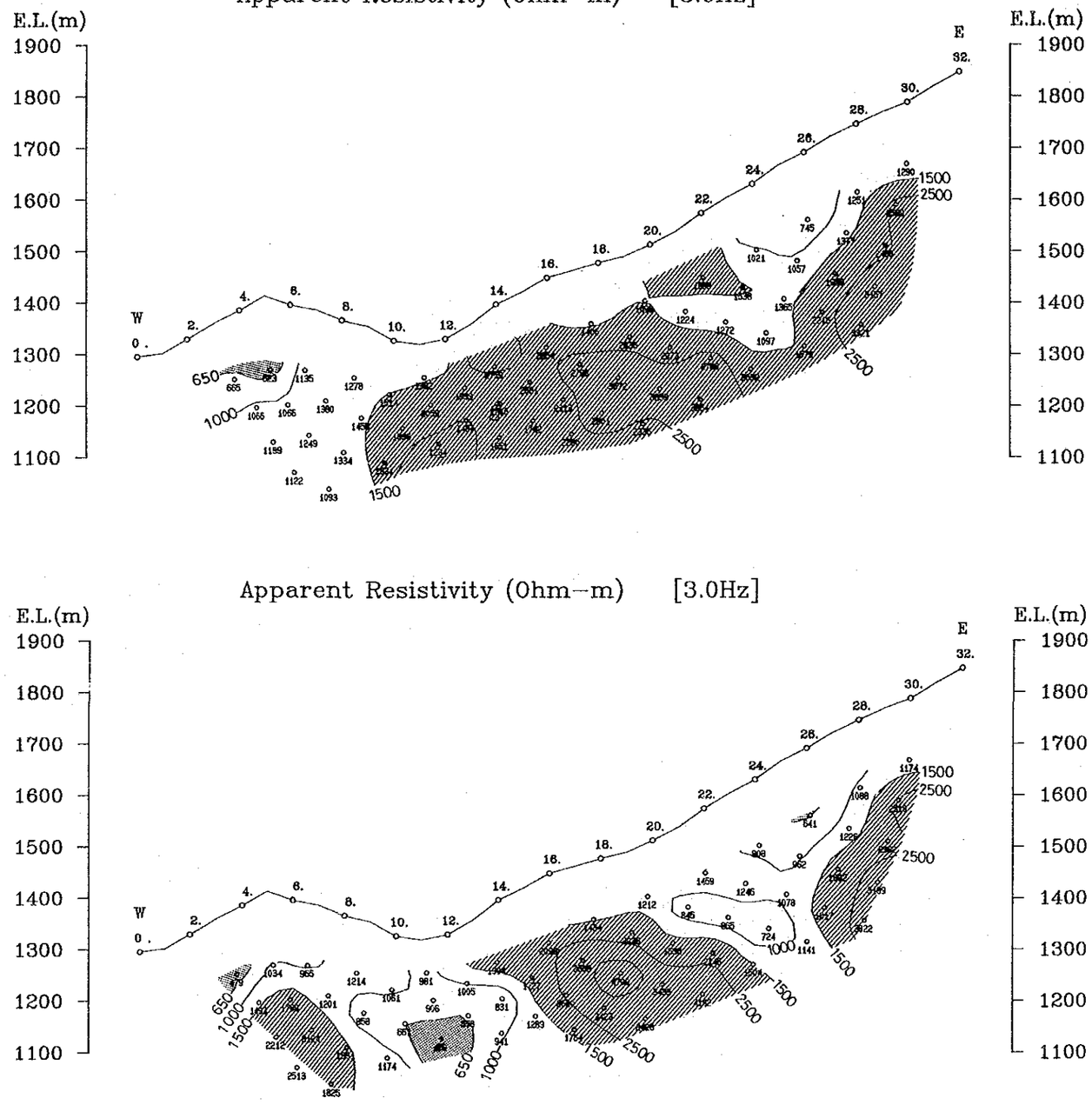

Fig. II-2-20 Example of topographical correction of the Osohuayco, Balzapamba area

Chapter 3 Chaso Juan area

The Chaso Juan area is situated 40 km north of the Balzapamba area. The access by road can be done from Balzapamba via Babahoyo (159 km), and takes about 3 hours by car. In this area, geological and geophysical surveys were conducted.

3-1 Geological Survey

3-1-1 Purpose of survey and survey method

The purposes of these surveys are to clarify the relationship between mineralization, geological structure and igneous activity, and to detect prosperous mineral showings by comprehensively studying the results of these surveys and existing data.

Before starting the surveys, the routes were selected based on the existing data. We used the topographic map at a scale of 1:5,000 which was especially prepared by INEMIN this time to prepare a route map. The results of surveys were summarized into a topographic map at a scale of 1:10,000 by using available aerial photographs. Simultaneously with the geological survey, was measured the magnetic susceptibility for each outcrop along the main routes using a portable magnetometer to investigate the relationship between mineralization and magetic susceptibility.

The location maps of samples used for various test analysis are shown in Figure A-1 at the end of this report and the results of test analysis are listed on tables in this Chapter and Appendixes at the end.

3-1-2 Geology

The area is underlain by the Macuchi Formation and granitic rocks which were emplaced in the Macuchi Formation (Plate II-3-1, Fig.II-3-1 and Fig.II-3-2)

(1) Macuchi Formation An

Macuchi Formation An is mainly distributed in small area at the northeastern corner, and further expands outside of and to the east and west of the area. In the north and west, it is exposed as xenolith in the granodiorite. This rock consists mainly of dark gray tight and massive pyroxene andesite lava and coessential tuff breccia. Coessential fine-grained tuff, which is considered to be contained therein, and boulders of dark gray siliceous sediment are also observed.

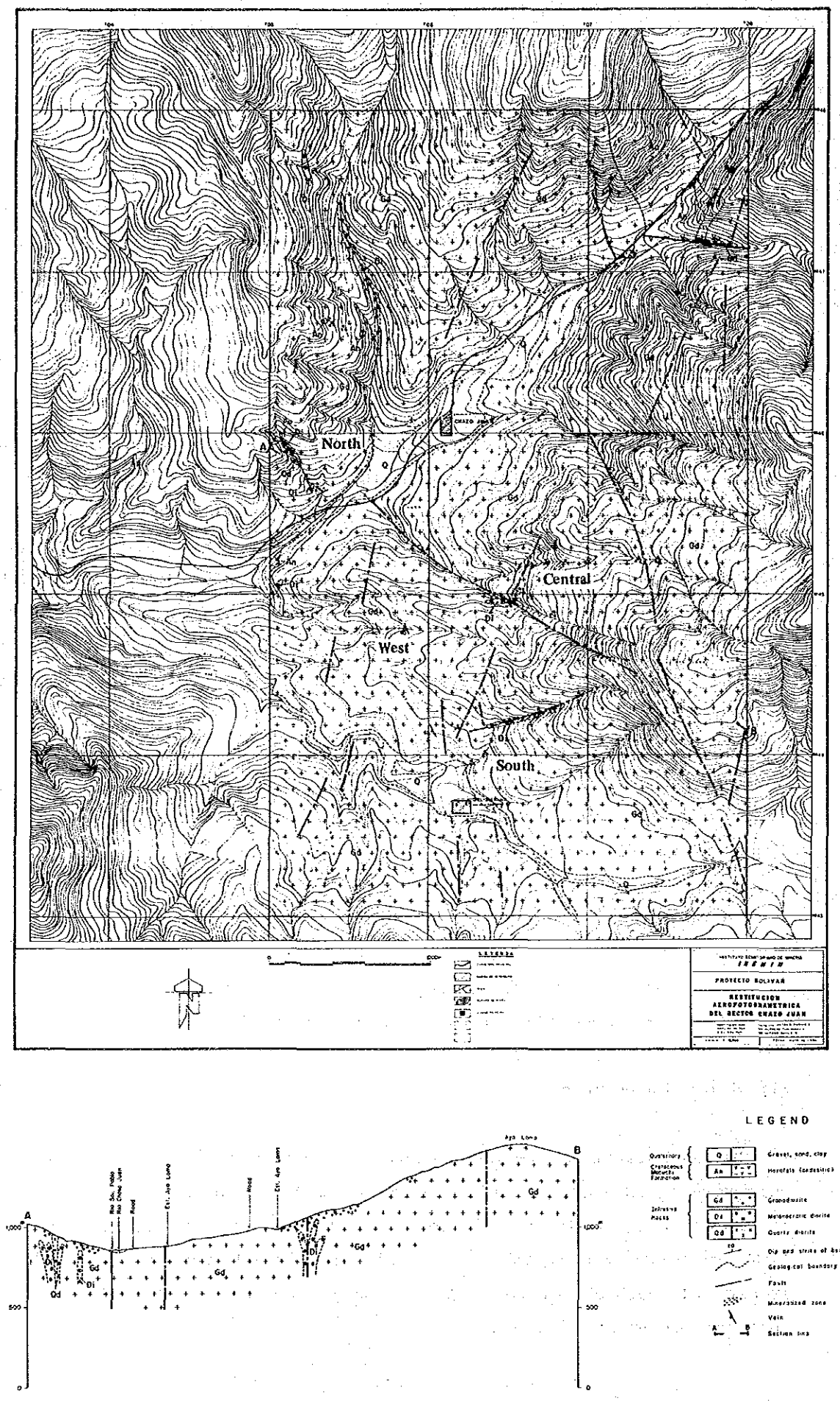

Fig. II–3–1 Geological map and distribution of mineral showings of the Chaso Juan area

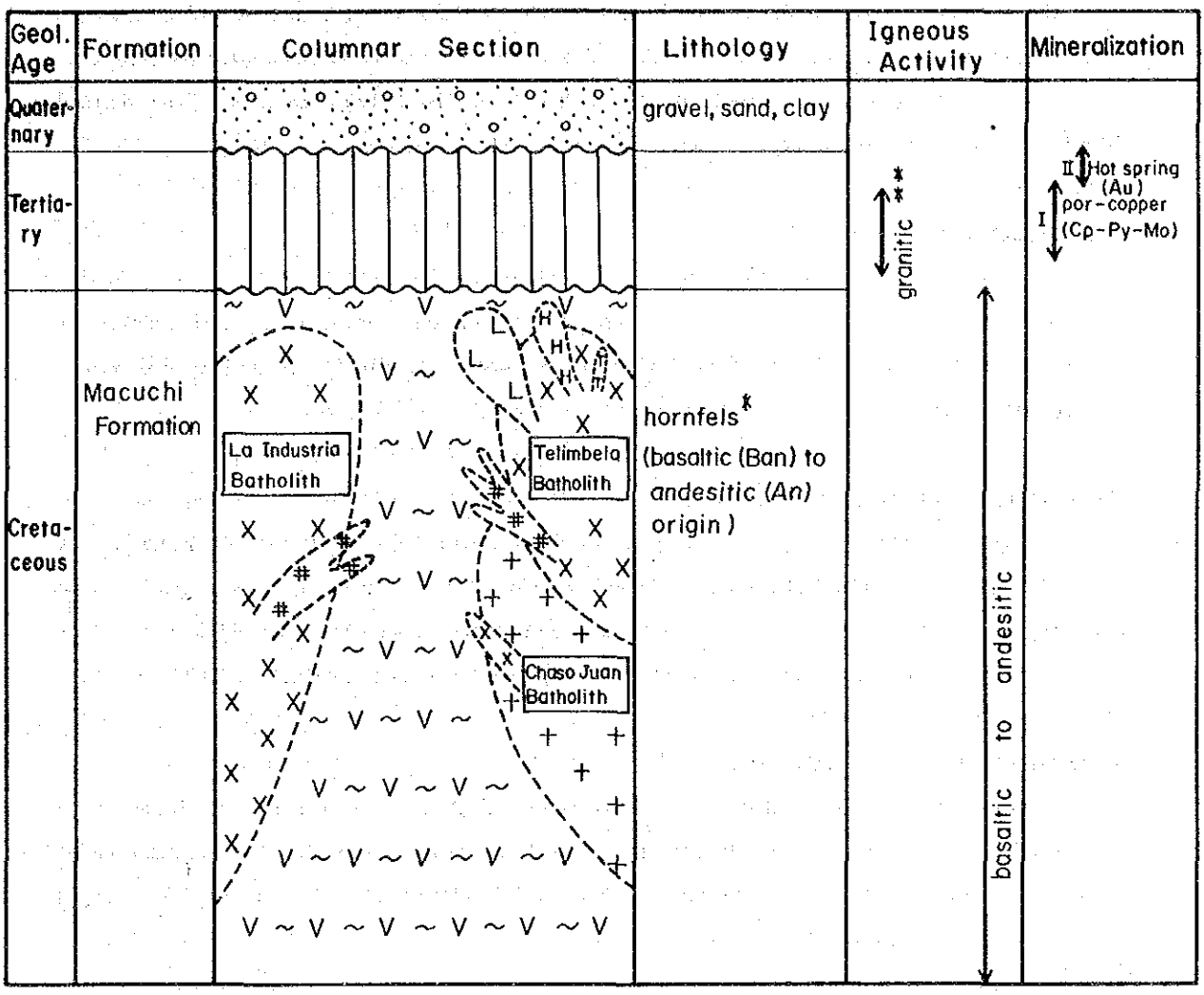

Granodiorite (Gd)

Quartz diorite (Qd)

Melanocratic diorite (Di)

Quartz porphyry (Qp)

Hornblende quartz diorite (HQd)

Porphyritic quartz diorite (PQd)

(Above-mentioned these rocks do not show the geological time of their intrusion but their occurrence)

* Chaso Juan : Andesitic (Th ≒ 400m)
Telimbela : Basaltic andesitic (Th ≒ 1,000m)

** Chaso Juan : 20.9 ± 0.7 Ma (Gd), 17.5 ± 0.6 Ma (Di)
La Industria : 25.5 ± 0.9 Ma (Qd)
Telimbela : 19.4 ± 0.6 Ma (Qd), 14.5 ± 3.0 Ma (HQd), 15.7 ± 1.0 Ma (Qp)

Fig. II–3–2 Generalized Stratigraphy in the Chaso Juan, Telimbela and La Industria-Yatubi areas

The Macuchi Formation An is mostly metamorphosed to hornfels, and original minerals and texture of source rock cannot be identified, but present hard and tight rock facies. They are locally similar to those of the Member A of the Balzapamba area. Fine-grained biotite, hornblende, pyroxene and quartz are observed.

(2) Granitic rocks

Granitic rocks are almost distributed in this entire survey area, and consist of hornblende-biotite granodiorite botholith (Gd), melanocratic diorite dike (Di) and quartz diorite dike (Qd).

1) Hornblende-biotite granodiorite (Gd)

Hornblende-biotite granodiorite (Gd) is almost distributed over the entire survey area. Lithology is holocrystalline and equi-granular (medium-grain to coarse-grain). The medium-grained dominates in the northeast and central parts (Central mineralized zone) of the survey area and toward the southeastern part, and the coarse-grained in other areas.

2) Melanocratic diorite dike (Di)

In melanocratic diorite dike (Di), were observed at least 7 rock bodies. Large quantities of these rock bodies are distributed around the mineralized zone. The direction of intrusive rocks are in the N-S trend or NE-SW to ENE-WSW trends. The with of dikes ranges from 20 to 50 m showing contacts irregur.

The distribution of dikes as follows:

① Northwest of survey area: 2 rock bodies
② West of survey area: 2 rock bodies
③ Western end of survey area: 1 rock body
④ Central part of survey area: 1 rock body
⑤ South of survey area: 1 rock body

For a rock body in ⑤, microscopic observation, age determination and analysis of entire rock were conducted. The microscopic characteristics of melanocratic granodiorite are as follows:

Biotite-hornblende diorite (A2009)

Location: 0.6 km north of Mulidiahuan, along the northern branches of river Rio Mulidiahuan

Texture: Partially porphyritic

Constituent minerals: Plagioclase>hornblende>biotite>quartz, apatite, opaque minerals

Alteration minerals: Biotite, chlorite > epidote

Biotite is locally affected by chloritization.

3) Quartz diorite dike (Qd)

Quartz diorite dike (Qd) has intruded into the northern mineralized zone and west of the survey area in NW-SE direction, and is a rock body 60 m long and 20 m wide.
This rock body has penetrated the melanocratic diorite dike (Di).

The melanocratic diorite dyke (A2009) is dated as 17.4±0.6 Ma by the K-Ar method (Table II-3-1) The hornblende-biotite granodiorite conducted in the first fiscal year was dated as 20±0.7 Ma by the K-Ar method.

The results of Chemical analysis for granitic rocks are listed on Table II-3-2 including analitical data of other areas which are mentioned later. SiO2-FeO*/MgO diagram and normative quartz-orthoclase-plagioclase triangular chart in Fig.II-3-3 and Fig.II-3-4 respectively. The former diagram (Fig.II-3-3) shows that most of granitic rocks are plotted in an area of calc-alkaline rock series while small scale intrusive rock body or dike are not always in the cale-alkaline rock series. The latter shows that they are all plotted in an area of granodiorite or quartz diorite.

(3) Geological structure

Structurally the area is emphasized by the NW-SE trend and E-W trend as the direction of individual mineralized zones, but the distribution of the mineralized zone shows N-S trend. The direction of dikes is in N-S, NW-SE and ENE-WSW.

Lineaments develop in the NNE-SSW, N-S, NE-SW, NW-SE and E-W direction. Among them, the central mineralized zone converges on the intersection of NNE-SSW trend and NW-SE trend, and the southern mineralized zone is situated at a position where NNE-SSW, NE-SW and N-S trends cross each other.

3-1-3 Mineralization and alteration

In the north, west, central and south of the chaso Juan area, porphyry-copper type mineralization is observed in granodiorite batholith. The features of mineralization can be cited as follows:

1) The mineralized zone consists of chalcopyrite-pyrite-(molybdenite) dissemination and veinlet zone.

Table II–3–1 Results of isotopic age determination (K-Ar method)

No.	Sample No.	Location		Rock Name	Sample Type	Potassium (K wt%)	Radiogenic ^{40}Ar (10^{-8} cc/g)	K-Ar Age (Ma)	Air Cont. (%)
		Coordinates							
		E	N						
1	A2009	Chaso Juan		hb-bt-q. dio	Whole Rock	1.00 ±0.03	68.1 ±0.9	17.5 ± 0.6	22.5
		706.40	9844.17						
2	C2016	Telimbela		bt gr porhyry	Whole Rock	0.82 ±0.05	50.1 ±0.7	15.7 ± 1.0	23.0
		702.53	9815.60						
3	C2062	Telimbela		hb-bt-q. dio	Hornblende	0.16 ±0.03	9.07 ± 0.40	14.5 ± 3.0	69.0
		705.15	9817.00						
4	A2076	Las Guardias		hb-bt dac	Hornblende	0.16 ±0.03	14.9 ±0.4	23.9 ± 4.8	52.6
		706.77	9802.10						
5	A2092	Las Guardias		hb-bt-q. dio	Hornblende	0.28 ±0.04	34.8 ±0.6	31.7 ± 4.8	39.4
		706.12	9802.64						

Table II–3–2 Results of chemical analysis of granitic rocks

No.		1	2	3	4	5
Sample No.		A2009	C2016	C2062	A2076	A2092
Area		Chaso Juan	Telimbela	Telimbela	Las Guardias	Las Guardias
Coordinates	E	706.40	702.53	705.14	706.77	706.12
	N	9844.17	9815.60	9817.00	9802.10	9802.64
Rock Name		hb-bt-q. dio	bt gr porhyry	hb-bt-q. dio	hb-bt dac	hb-bt-q. dio
Chemical Composition	SiO_2	63.44 %	63.63 %	59.33 %	65.09 %	52.85 %
	TiO_2	0.41	0.49	0.60	0.35	0.62
	Al_2O_3	16.59	16.61	18.19	16.29	15.78
	Fe_2O_3	3.05	3.33	4.13	3.53	4.17
	FeO	2.51	1.97	2.60	1.93	4.60
	MnO	0.11	0.09	0.22	0.12	0.21
	MgO	2.33	1.59	2.50	1.89	7.86
	CaO	5.41	3.51	6.64	5.60	8.91
	Na_2O	3.38	3.78	3.43	3.19	2.14
	K_2O	1.43	1.04	0.34	0.62	0.69
	P_2O_5	0.10	0.13	0.16	0.07	0.08
	Ig-loss	1.18	3.47	1.05	1.19	1.63
	Total	99.94	99.64	99.19	99.87	99.54
CIPW Normative Minerals	q	22.92	28.04	20.22	29.42	7.84
	c	0.00	3.20	0.49	0.36	0.00
	or	8.33	6.15	2.01	3.66	4.08
	ab	28.60	31.99	29.02	26.99	18.11
	an	25.93	16.56	31.90	27.32	31.41
	ne	0.00	0.00	0.00	0.00	0.00
	ac	0.00	0.00	0.00	0.00	0.00
	ns	0.00	0.00	0.00	0.00	0.00
	ks	0.00	0.00	0.00	0.00	0.00
	wo	0.00	0.00	0.00	0.00	0.00
	diwo	0.11	0.00	0.00	0.00	5.12
	dien	0.08	0.00	0.00	0.00	3.78
	difs	0.02	0.00	0.00	0.00	0.84
	hyen	5.73	3.96	6.23	4.71	15.79
	hyfs	1.62	0.23	0.79	0.27	3.59
	olfo	0.00	0.00	0.00	0.00	0.00
	olfa	0.00	0.00	0.00	0.00	0.00
	mt	4.42	4.83	5.99	5.12	6.05
	hm	0.00	0.00	0.00	0.00	0.00
	il	0.78	0.93	1.14	0.66	1.18
	tn	0.00	0.00	0.00	0.00	0.00
	pf	0.00	0.00	0.00	0.00	0.00
	rn	0.00	0.00	0.00	0.00	0.00
	ap	0.23	0.30	0.37	0.16	0.19
	cc	0.00	0.00	0.00	0.00	0.00
	pr	0.00	0.00	0.00	0.00	0.00
	Total	98.76	96.17	98.15	98.68	97.98

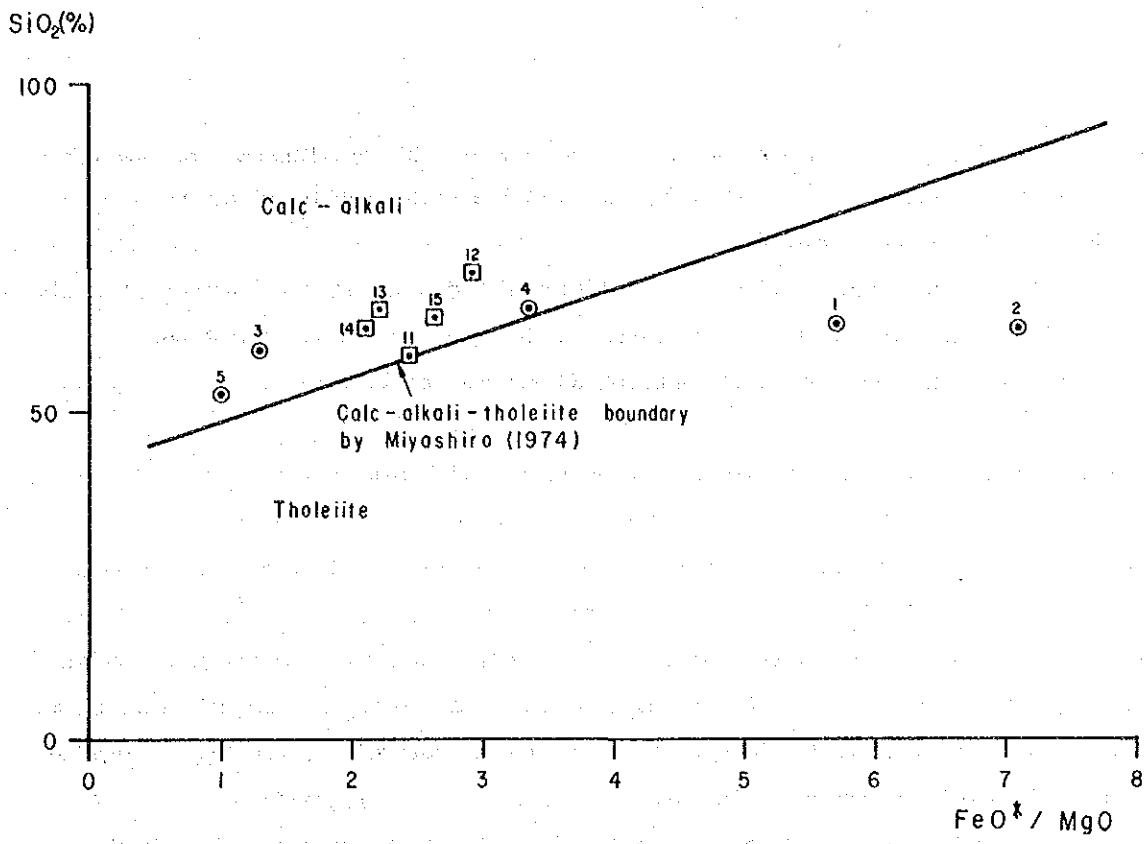

I : A2009 , 2 : C2016 , 3 : C2062 , 4 : A2076 , 5 : A2092

II : A1131 , 12 : B1109 , 13 : C1079 , 14 : B1166 , 15 : B1071

Fig. II–3–3 Chemical variation diagram for granitic rocks: SiO_2 - (FeO*/MgO) variation diagram

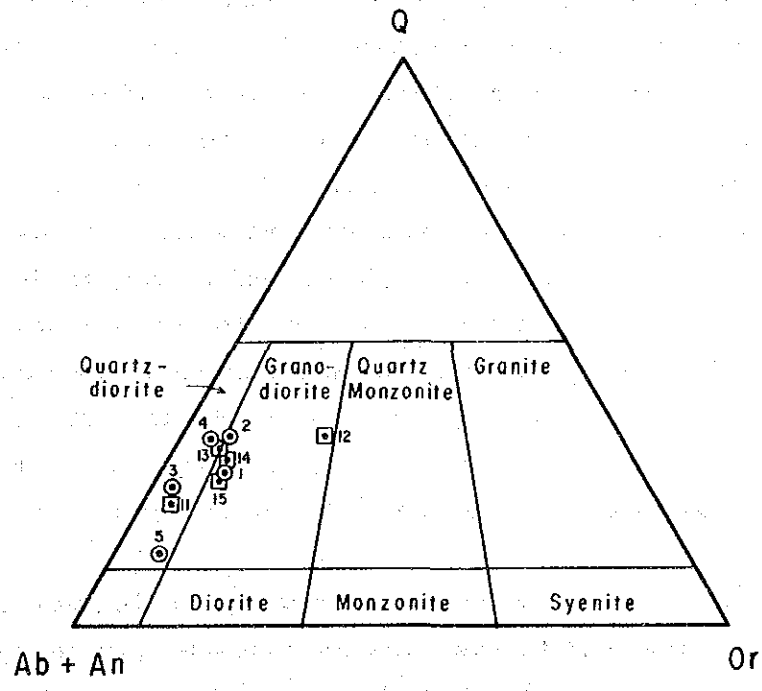

I : A2009 , 2 : C2016 , 3 : C2062 , 4 : A2076 , 5 : A2092

II : A1131 , 12 : B1109 , 13 : C1079 , 14 : B1166 , 15 : B1071

Fig. II–3–4 Chemical variation diagram for granitic rocks: normative quartz (Q) - orthoclase (Or) - plagioclase (Ab+An) diagram

2) Chalcopyrite/pyrite ratio of the mineralized zone is higher than that of any other mineralized zones in the Bolivar area, though with a small quantity of pyrite
3) Chalcopyrite is large grained.
4) Alteration of host rock varies among each mineralized zone and is characterized mainly by silicification and biotitization. Some are characterized by chloritization.
5) Direction of individual veinlets is in NW, NE and E-W trends.

The occurrence of major mineralized zones is as follows:

(1) North mineralized zone

The North mineralized zone is situated in tributary of San Pablo valley. Mineralized zones are 10 to 50 m wide over 400 m long and scattered in granodiorite and melanocratic diorite at three places. In these mineralized zones, observed are chalcopyrite-pyrite-(molybdenite) veinlets and dissemination.

The analytical results of the ore samples show 1.3 g/t in Ag, and 0.10 % in Cu. Noticeable alteration is observed in secondary biotite.

(2) West mineralized zone

The West mineralized zone is situated 10 km southwest of Chaso Juan. The mineralized zone is chalcopyrite and pyrite dissemination and veinlet zone in coarse-grained granodiorite which is affected by strong silicification. The width of the outcrop is 25 m, and the mineralized zone shows N20°W in strike, and 40°S in dip. Disseminated sulfide minerals mainly occur in the portion of mafic minerals.

The analytical results of the ore samples show 0.1 g/t in Au, 1.7 g/t in Ag and 0.24 % in Cu. For alteration, silicification is conspicuous, and secondary biotite is common. Large quantities of limonite veins of 2 to 3 cm wide are observed for about 200 m on the downstream side of this outcrop. The mineralized zone shows N20° to 40°W in strike, and 40° to 55°S in dip.

(3) Central mineralized zone

The Central mineralized zone (the east mineralized zone of the Phase I survey) is situated in the middle reaches of Aya Loma valley and its branches , extending over 600 m x 400 m, and mineral showings are scattered at eleven places. The mineralized zone consists of chalcopyrite and pyrite dissemination and veinlet in zone of melanocratic granodiorite

and granodiorite. Molybdenite is locally observed in veinlets. Major mineralized zone is observed for 150 m along the valley. Veinlets of the mineralized zone show N80°W in strike, and 60°S in dip.

The analytical results of the ore samples show 0.1 g/t in Au, 4.2 g/t in Ag, and 1.41 % in Cu at maximun. As a result of microscopic observation of sample No.A2017, chalcopyrite-pyrite-magnetite-molybdenite is observed in quartz veinlets (3 mm wide) and in host rock.

Host rock is affected virtually by chloritization and epidotization. The former is widely observed in the mineralized zone, and the latter tends to dominate in a portion where large quantities of chalcopyrite are present in the mineralized zone. By X-ray diffractive analysis for the latter, potassium feldspar and secondary biotite are locally detected. In the eastern upper stream side, white alteration zone accompanied with pyrite extends over 50 m in N70°E direction along the river.

(4) South mineralized zone

The South mineralized zone is situated in the northern part of Mulidiahuan. This mineralized zone extends over an are of 800 m x 300 m, and the east of the mineralized zone shows different occurence from the west. In the east of the mineralized zone, chalcopyrite-pyrite dissemination and veinlet zone occur in coarse-grained granodiorite. A mineralized zone is observed for about 300 m along the valley in the southwest direction.

The analytical results of the ore samples show 0.1 g/t in Au, 7.6 g/t in Ag and 1.46 % in Cu at maximum. The host rock is affected by silicification and weak chloritization. White alteration rocks are present locally.

In the west of the mineralized zone, two rows of chalcopyrite-pyrite veinlet zones in small cracks of coarse-granodiorite are distributed with intervals of about 100 m. The veinlet (about 1 to 10 cm of vein width) shows N20° to 30°W in strike, and 45° to 65°S in dip.

The analytical results of the ore samples show 1.5 g/t in Au, 160.9 g/t in Ag and 9.03 % in Cu at maximum. The host rock is affected by weak silicification.

In addition, chalcopyrite-pyrite dissemination and veinlet zones are observed at four places, in the northeast of the survey area, but each of them is small in scale.

3-1-4 Results of magnetic susceptibility measurement

To determine quantitatively demagnetization due to mineralization, magnetic susceptibility was measured, using a portable magnetometer. This measurement was made through the

area. The magnetometer was Kappameter Model KT-5 of Czechoslovakia with measurement susceptibility of 1 x 10^{-3} SI units.

At the measurement, efforts were made to completely scrape weathered portions off from outcrops and to plane surface smooth to prevent measuring errors due to weathering and surface unevenness. Each measurements are the average of three values disregarding the highest and lowest ones (Table A-5).

Measurement values sharply fluctuated from 0.04 to 137 x 10^{-3} SI units depending on the outcrop. Fresh granodiorite showed 20 to 40 x 10^{-3} SI units, melanocratic diorite, 40 to 137 x 10^{-3} SI units, andesite lava in the Macuchi Formation, 50 to 70 x 10^{-3} SI units, quartz-bearing andesite lava, tuffs, and sedimentary rocks (Las Guardias area) in this formation, all less than 10 x 10^{-3} SI units. Main mineralization in this area was porphyry copper type. Taking into consideration the results of the previous year and with values below 20 x 10^{-3} SI units as anomalously low, each anomalous values for low magnetic susceptibility were set as follows: 0.1 to 5.0 x 10^{-3} SI units as extremely low; 5.1 to 10.0 x 10^{-3} SI units as low considerably; 10.1 to 20.0 x 10^{-3} SI units as low, and more than 20.1 x 10^{-3} SI units as background. Based on these four anomalous values, an analytical chart for anomalous zones was prepared (Fig.II-3-5).

Anomalous zones for magnetic susceptibility are found at four places. These anomalous zones consist of a zone extending in N-S direction from the Central mineralized zone to the South mineralized zone, zones detected in the Northern and West mineralized zones, and zones detected in mineral showings in the northwestern and northeastern zones. All of these anomalous zones are associated with mineralization. The scale of the foremost former anomalous zone is as intense as that of the anomalous zone detected in the El Torneado mineralized zone of Balzapamba area. The other anomalous zones are small in scale. As described above, magnetic susceptibility measurement was highly effective in understanding the scale of mineralization.

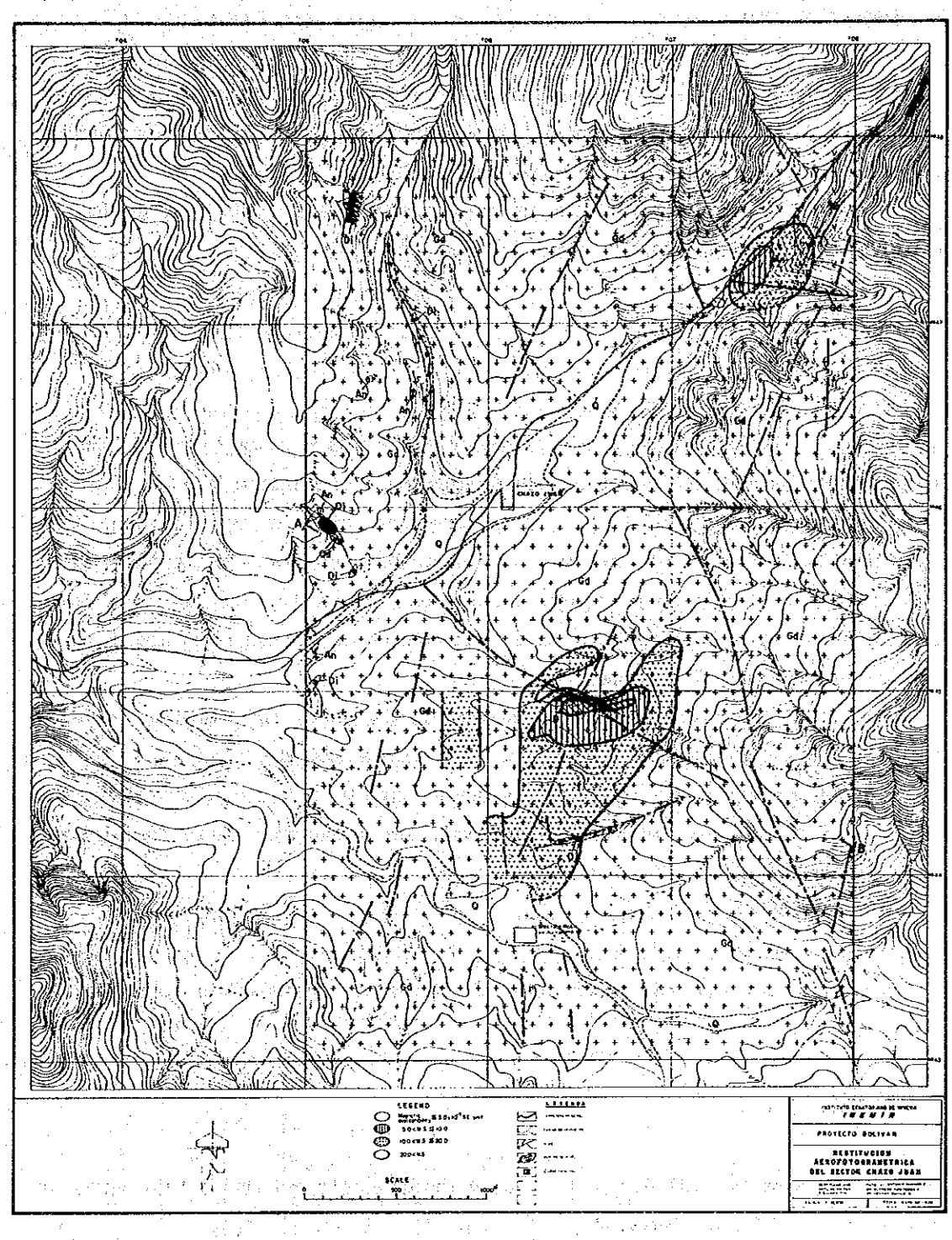

Fig. II–3–5 Interpretation map of magnetic susceptibility of the Chaso Juan area

3-2 Geophysical survey

3-2-1 Purpose of survey

The detailed geological survey was carried out on several mineral showings confirmed by the Phase I survey, and a promising mineralized zone was selected for further exploration work by means of IP method geophysical survey.

The purpose of the survey is to investigate the possible existence of the ore deposits there by a conventional IP method.

3-2-2 Survey method

(1) Measurement method

The measurements were done by the frequency domain method using 3.0Hz and 0.3Hz in a dipole-dipole electrode configuration with a separation factor n from 1 to 5.

The geological results of the first phase survey and this year survey concluded that the Wast and South mineralized zones were promising. Therefore, this survey was carried out in order to clarify the existent correlation between the East and the South mineralized zones as well as to find the distribution of mineralization at the depth of the above mentioned mineralized zones.

Based on the investigated geological structure, six survey lines with an extension 1,600m each were set along a S60° E direction and keeping a 300m line spacing.

The numbering of the measuring stations was set from 0 to 32 from the northwest end of every line to southeast with a 50m interval. The measurements were done between stations spaced 100m with a 100m potential electrode.

(2) Survey instruments

Instruments used for the conventional IP survey are described in item 2-2-2 of Chapter 2.

3-2-3 Analysis method

The details of the method used to analyze the data obtained during this survey is described in item 2-2-3 of Chapter 2.

3-2-4 Results of survey and analysis

The observed resistivities range from 412 to 7,130 Ohm-m. As a matter of convenience, the resistivity range will be defined here as follows:

High : more than 2,500 Ohm-m

Middle: from 1,000 to 2,500 Ohm-m

Low: less than 1,000 Ohm-m

The FE values will also be defined as follows:

High: more tan 5%

Middle: from 3 to 5%

Low: less than 3%

On the surveyed area, granitic rocks are predominantly seen and therefore, the variation in FE and apparent resistivity due to a difference in rock facies should be small. As a result, low resistivity changes are due to alteration and weathering, whereas high resistivity changes are due to silicification.

On the other hand, FE values are useful information as they also depend on the sulphide content.

The data used for pseudo-section and map interpretations were corrected topographically in order to make them more realistic and reliable

(1) Results of electric measurement of rocks

In the Chaso Juan Area, eight rock samples were collected from the surface and subjected to laboratory determinations in resistivity and FE. The results are shown on Table II-3-3.

Table II -3-3 Resistivity and FE of Rock Samples in Chaso Juan Area

No.	Sample No.	Rock Name	Occurrence	ρ (Ω·m)	FE (%)
1	C 2009	co hb-bi gd	cp-py diss	5,490	3.5
2	B 2004	dark gray mela. di	py diss	1,810	2.8
3	A 2015	granodiorite	cp-py diss/film	9,170	14.0
4	C 2002	black fine hornfels	cp-py diss	6,280	2.5
5	C 2001	sili. andesite	py-qtz vein/ntwk	3,100	1.6
6	C 2006	and tf bre	cp-py diss	572	4.8
7	D 2002	melanocratic diorite	py diss	6,650	3.8
8	D 2007	med ~co bi-hb gd	cp-py film	6,550	6.3

(2) Plan maps

1) n=1 (Figs.II-3-7 and II-3-8)

a) Apparent resistivity plan map (Fig.II-3-7)

Apparent resistivity values range from 412 to 4,370 Ohm-m. These values give indications of being high in the northeastern part and low in the south and west. The contour pattern trends approximately along the N-S to NE-SW direction.

The map indicates six low resistivity anomaly zones, named from A to F, and two high resistivity zones named as P and Q.

Low resistivity zones C, D, E and a part of zone F are interpreted as correlated to argillization associated with mineralization in the central and southern mineralized zones and with part of an inferred fault.

The low resistivity zones A, B and F may not be related to mineralization, but rather related to weathering and alteration, however, the high resistivity zones P and Q on the Line C2 correspond to the central mineralized zone and indicate silicification.

The middle resistivity over 1,500 Ohm-m at station 6 on Line C4 corresponds to the western mineralized zone. Another middle resistivity zone which is found distributed along a direction oriented N-S to NE-SW from Lines C4 to C5, may indicate silicification related to mineralization.

b) FE plan maps (Fig.II-3-8)

FE values range from 1.8 to 5.8%. A middle FE zone of more than 3% is widely distributed in the northeastern and southwestern part in the area and two high FE zones are located at around station 3 (anomaly 1) and station 15 (anomaly 2) on Line C4.

The FE anomaly I of more than 4%, which extends from Line C3 to Line C6 conforming a long and stretched distribution, corresponds to the western mineralized zone. Another FE anomaly I of more than 4%, is located between the central and southern mineralized zone. The S3 mineralized zone corresponds to this anomaly.

A moderate FE anomaly at the east end of Line C2 corresponds to the central mineralized zone C6.

2) n=3 (Figs.II-3-9 and II-3-10)

a) Apparent resistivity plan map (Fig.II-3-9)

Resistivities are seen on this map ranging from 611 to 5,160 Ohm-m. In general, these values are higher than those at n=1.

Since the low resistivity anomalous zones A and C disappear in this map, it can be interpreted that the anomaly is due to a thin layer on the surface. On the other hand, the low resistivity zones B, D and E, which show a half shape of the pants-leg pattern anomaly, are seen separated by three zones of higher resistivity. The central one is associ-

ated with mineralization.

The high resistivity anomalous zones P and Q become wider and incrementing their resistivity. It means that the scale of the resistive rocks becomes bigger at depth. Two other high resistivity anomalous zones R and S appeare in the central part, which correspond to the lower part of a moderate high anomaly more than 1,500 Ohm-m apparent resistivity.

b) FE plan map (Fig.II-3-10)

FE values used in this map ranges from 1.5 to 6.2%. Its magnitude become bigger in this map, with the exception of the ones found in the northern part.

The scale of the anomalies **1** and **2** become bigger. The IP anomaly **1** seems to be separated in two parts. East FE anomaly is considered to be another one which may belong to the IP anomaly **2**.

3) n=5 (Figs.II-3-11 and II-3-12)

a) Resistivity plan map (Fig.II-3-11)

Resistivities in this map (1,050 to 7,130 Ohm-m) are seen their values increased as compared with those at n=3.

All low resistivity anomalies vanish in this map. The middle resistivity zone of less than 1,500 Ohm-m, which seems to conform a pants-leg pattern anomaly, is distributed in the central and southern part of the area.

The high resistivity anomalies P and Q widen their distributions in this map and merge with the high resistivity anomaly R. Two new high resistivity anomalies, T and U, appear in this map.

b) FE plan map (Fig.II-3-12)

FE values are seen to vary in this map from 1.8 to 7.4%. The magnitude of FE in the the anomaly **1** becomes bigger and a new anomaly **3** appears at station 11 on Line C6. This anomaly is interpreted to be indicative of the depth of mineralization of the South mineralized zone.

(3) *IP* pseudo-sections

1) Line C1 (Fig.II-3-13)

The resistivity values vary here from 751 to 7,130 Ohm-m and FE values from 1.8 to 3.8%.

The anomalies P and Q are interpreted as a resistive body at depths of the stations 10 to 17 and 20 to 26.

There seems to be a tendency in FE to gradually decrease from east to west. No anomalous source is expected.

2) Line C2 (Fig.II-3-14)

The resistivity values change from 537 to 5,300 Ohm-m and FE values from 0.7 to 4.4%.

As same as in Line C1, a resistive body is also inferred at the depths from stations 7 to 16 and from 20 to 28.

Although there exists the same resistivity tendency as that on Line C to decrease westwards, the variation rate is bigger in this line.

Two weak FE anomalies at stations 19 and 30, correspond to the middle mineralized zones C2 and C3, and C5, respectively.

3) Line C3 (Fig.II-3-15)

Resistivity ranges from 469 to 4,370 Ohm-m and FE 2.1 to 6.1%.

The high resistivities detected at the depths of stations 6 to 8 and 16 to 22 correspond to the anomalies P and Q, while the high resistivities at the depth of 10 correspond to the anomaly R. These high resistivities indicate the existence of silicified bodies at the depths.

The low resistivity anomalies C and D in the eastern part of the Line seem to be due to a thin layer located at stations 18 to 20 and at station 24, respectively. Similar anomalies conforming a pants-leg anomaly pattern are detected at stations 5, 10, 13, 17, 19, 21 and 25. Since these anomalies are located in the vicinity of high resistivities, they are likely to be due to some silicification process in the rocks.

4) Line C4 (Fig.II-3-16)

In this section, the resistivity changes from 583 to 3,380 Ohm-m and FE from 2.7 to 7.4%.

High resistivity reflecting the high resistivity anomalies R, T, S and U are seen distributed at the middle-deep portion. The high resistivity anomalies P and Q are combined to the anomaly R. The half shape of a pants-leg low resistivity pattern near station 17 and corresponding to the anomaly E indicates the existence of a low resistivity layer in the vicinity of 18.

Similar anomalies to the pants-leg pattern are detected centered at the stations 3 (anomaly 1), 10, 12, 15 and 17 (anomaly 2). Although no mineralization evidence is observed at surface, these anomalies seem to be related to mineralization.

5) Line C5 (Fig.II-3-17)

Resistivity values vary from 422 to 3,460 Ohm-m and from FE 1.8 to 5.5 %, showing a complicated distribution due to the superposition of pants-leg pattern anomalies induced

by a low resistivity layer on the surface. Pants-leg pattern anomalies are seen at station 9, 13 and 17.

FE values tends to decrease gradually to the east. Several FE anomalies are recognized in this line.

Pants-leg pattern shallow anomalies are seen centered at stations 4, 8, 13, 15(n=3), 18 and deep anomaly at station 15. Since the anomalies at stations 13 and 18, which correspond to the southern anomalies S2 and S3 respectively, detected the mineralizated zones, other anomalies may also indicate mineralization.

6) Line C6 (Fig.II-3-18)

Resistivity values changes from 412 to 2,050 Ohm-m and FE values from 2.3 to 5.1%.

Both resistivity and FE show in general a uniform distribution with the exception of FE distribution around station 11 (anomaly 3) and on the east end (station 31) of the survey line.

Low resistivity is found at shallow depth below station 19.
Resistivity generally increases in proportion to depth to the east with a monotonous inclination that can be interpreted with a high resistivity body at shallow depth in the west and another at depths in the east. Low FE values of less than 3% are observed around station 19. Like resistivity, FE increases in proportion to depth to the east, interpreting these results as a two layer structure dominant in this line, and presenting low resistivity and low FE at the shallow part and high resistivity and high FE at depth.

(4) Simulation analysis

Simulation analysis was carried out between stations Nos.0 and 20 on Line C4 crossing the IP anomalies I and II, and between 22 and 32 on Line C2 crossing the central mineralized zone.

The results are shown in Figs.II-3-19, and II-3-20.

1) Line C4 (Fig.II-3-19)

Judging that average resistivity is 2,000 Ohm-m and FE is 4.5%, the background body (Block No.1) was assumed as having 2,000 Ohm-m and 4.5%. Also from the tendency shown by the resistivities which increase toward depth, a relatively resistive body (Block No.2) having 4,500 Ohm-m with an 4.5% of FE was assumed at the depth.

A low resistivity layer assumed at the surface between stations 6 and 18, with 30-70m in thickness and 800 to 1,400 Ohm-m in resistivity, may correspond to a weathered layer or a weakly argillized zone. With the exception of the FE values seen in this layer, Blocks Nos.11 and 12 range from 2.8 to 4.5% which are less than the background FE 4.5%. Blocks